Research report 2011:03

Particle Image Velocimetry: Fundamentals and Its Applications

MOHSEN JAHANMIRI

Division of Fluid Dynamics
Department of Applied Mechanics
CHALMERS UNIVERSITY OF TECHNOLOGY
Göteborg, Sweden, 2011

Particle Image Velocimetry: Fundamentals and Its Applications

MOHSEN JAHANMIRI

Research report 2011:03
ISSN 1652-8549

Division of Fluid Dynamics
Department of Applied Mechanics
CHALMERS UNIVERSITY OF TECHNOLOGY
SE-412 96 Göteborg
Sverige
Telephone +46 (0)31 772 1000

Particle Image Velocimetry: Fundamentals and Its Applications

Mohsen jahanmiri

Dept. of Applied Mechanics, Chalmers University of Technology
Göteborg, Sweden
&
Dept. of Mech. and Aerospace Engineering, Shiraz University of Technology
Shiraz, Iran

Abstract

Particle image velocimetry (PIV) is the newest entrant to the field of fluid flow measurement and provides instantaneous velocity fields over global domains. As the name suggests, PIV records the position over time of small tracer particles introduced into the flow to extract the local fluid velocity. Thus, PIV represents a quantitative extension of the qualitative flow visualization techniques that have been practised for several decades. This paper gives a brief background on evolution of PIV and then its principle of operation, main features and basic elements are explaind. Errors in PIV occurring while measurements are discussed and, the state-of-the-art of the technique today is overviewed and illustrated by reference to recent, seminal publications describing both the development and application of PIV.

Introduction

Some of the earliest quantitative velocity measurements in fluid flows were obtained using Pitot-static tubes. The subsequent introduction of hot-wire anemometers in the 1920s (Prasad, 2000) was a significant advance, especially in terms of probe miniaturization, frequency response, and the ability to measure multiple velocity components. However, both these techniques require the insertion of a physical probe which can intrude on the flow itself. The invention of the laser in the 1960s led to the development of the laser- Doppler anemometer which uses a laser probe to enable non-intrusive velocity measurements. Despite the rapid strides in the design of such systems, and the great sophistication of the associated electronics, one cannot escape the fact that all these techniques are at best "*point-wise*", i.e. the velocity information is obtained only at the point occupied by the probe. While these techniques continue to retain an important position in an experimentalist's arsenal, the ability to make "*global*" velocity measurements has elevated particle image velocimetry (PIV) to a special status in fluid mechanics.

Particle image displacement velocimetry (PIDV) or, as it is now most often called, particle image velocimetry (PIV) comprises a class of flow measuring techniques that are characterized by the recording of the displacement of small particles embedded in a region of a fluid. Although these techniques are still developing, a number of excellent review papers have already been published, of which we may mention those of Lauterborn and Vogel (1984), Dudderar et al. (1988), Adrian (1986, 19991), Buchhave, (1992), Grant (1997) and Prasad (2000), which together describe the historical development, measurement technique, and applications of PIV.

The principle behind a PIV system is simple: The flow is illuminated by a strong light source, and the particle positions are recorded by imaging the light scattered from tracer particles onto a recording medium such as a photographic film or a matrix detector. Methods based on molecular scattering such as laser-induced fluorescence and methods based on Raman scattering are thus excluded. By concentrating on methods in which light is scattered simultaneously from a relatively large region of the fluid, the "whole flow-field," in contrast to a measurement in a relatively small region, a "point," we exclude the standard laser anemometric techniques such as laser-Doppler anemometry (LDA) and laser two-spot anemometry (LTA) and emphasize the whole-flow-field aspect of the measurement. Using this definition of PIV we thus

deal with an optical technique whose only material aspect is the presence of seed particles in the fluid. We may thus cite the usual advantages of optical techniques for flow measurement, in particular the noninterference with the flow. In practice the optical method may interfere considerably with the flow through the requirements of optical access and the need for optical windows in the structures surrounding internal flows. As the particles are expected to trace the motion of the fluid and at the same time act as transmitters of information in the form of scattered light, they must, of course, be present in the fluid in sufficient concentration and have the right size to be able to play both roles. Thus the choice of seed particles and the methods for their deployment in the fluid are important aspects of the PIV technique. One of the reasons for the interest in PIV is the current emphasis on research into coherent structures in turbulence-generating flows such as free shear flows and boundary layers. Another reason is the fact that the purpose of many flow measurements is to gain information on the gross flow pattern in a whole region or cross section of the flow and the PIV technique is able to provide this kind of information much faster or at least with less data collection time than conventional point methods. In many instances this reduction of measurement time can be of great economic benefit, especially in large flow facilities that are expensive to run. As we shall see, this savings in measurement time may also have its costs; often the PIV technique leads to a considerably increased processing time, the time it takes for the recorded data to be processed to yield velocity data. The long processing time may lead to a subsequent lack of "feel" for the progress of the measurement.

As mentioned by Buchhave, (1992), the PIV technique may be an efficient way of measuring the gross velocity structures of a flow region. However, as a measurement technique PIV will, of course, be compared to the "complementary" types of velocimetry, LDA and LTA, and further on to hot-wire anemometry. The interest naturally focuses on the question of how accurate, how fast, and how versatile the PIV technique is in comparison to these methods when the task is the measurement of traditional fluid mechanic quantities such as mean and rms velocities, temporal and spatial velocity moments, and various velocity correlations.

PIV may be said to be a consequence of the development of flow visualization techniques, which have contributed so importantly to the understanding of fluid flow phenomena. Flow visualization probably always played an important role in the study of fluid motion. The visual information about the development of structures in naturally occurring flows such as rivers or clouds is mentally stimulating, and it is straightforward to try to extend this type of visual input for the brain to flows that cannot be directly observed either because there is not enough visually observable contrast between the different regions of the flow or because the phenomena occur too fast to register in the human visual system. Thus began the development of methods of making fluid flows visible by the addition of various tracer agents to the flow and methods of recording fast-changing structures so that later they could be displayed at a comprehensible speed.

The problem with flow visualization as a tool for fluid mechanics is that the visual information provided by the images or sequences of image is not sufficient for the verification of theories of turbulence or for the evaluation of mathematical models of turbulent flows. Such applications require extensive quantitative information about the fluid velocities, not just at a single point but at two or more points in the flow-field at the same time. The conventional methods of acquiring spatial information invoke the Taylor hypothesis and use a time record of the velocity at a single point or employ two hot-wire probes or two separate laser anemometer systems to measure at two points simultaneously. Either way, the goal is to explore the spatial velocity correlations in a region of the flow by positioning the two measurement points at all possible pairs of points in the region. These methods, of course, allow determination of only the second-order correlations and moreover require stationarity, thus excluding a whole class of non-stationary or transient phenomena.

The extension of flow visualization methods to the acquisition of quantitative data took a giant step forward with the invention of image digitization methods and the development of image processing software. It is now possible by means of various image processing techniques to

identify structures in a turbulent flow and to follow these structures in time through processing of the digitized images. This way the researcher obtains quantitative information on the development of the flow. However, previously these methods were very difficult to employ, and, in particular, the unambiguous definition of a "structure" was presenting great difficulties, which resulted in uncertainties in the measurement. The "structure" itself undergoes changes as the flow develops. The additional step of adding particles to the fluid and attempting to track the particle motion then becomes a natural development, and the ambiguity in tracing a two-dimensional recording of a three-dimensional structure is replaced by the problem of identifying a dual or multiple particle image on a multiply exposed recording or identifying a particular particle from frame to frame in a multi-frame recording. However, once this task is accomplished, the advantage of the particle displacement method is that the measurement is well defined and does not suffer from any ambiguity due to changes in the structure whose development is to be studied.

Principle of operation

The experimental setup of a PIV system typically consists of several subsystems. In most applications tracer particles have to be added to the flow. These particles have to be illuminated in a plane of the flow at least twice within a short time interval. The light scattered by the particles has to be recorded either on a single frame or on a sequence of frames. The displacement of the particle images between the light pulses has to be determined through evaluation of the PIV recordings. In order to be able to handle the great amount of data which can be collected employing the PIV technique, sophisticated post-processing is required.
Figure 1 briefly sketches a typical setup for PIV recording. Small tracer particles are added to the flow. A plane (light sheet) within the flow is illuminated twice by means of a laser (the time delay between pulses depending on the mean flow velocity and the magnification at imaging). It is assumed that the tracer particles move with local flow velocity between the two illuminations. The light scattered by the tracer particles is recorded “via a high quality lens” either on a single frame (e.g. on a high-resolution digital or film camera) or on two separate frames on special cross-correlation digital cameras. After development the photo-graphical PIV recording is digitized by means of a scanner. The output of the digital sensor is transferred to the memory of a computer directly.

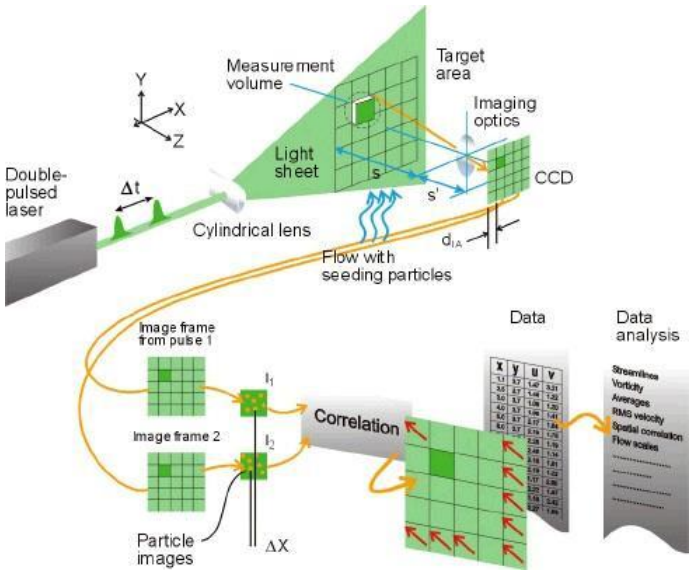

Figure 1: Experimental arrangement for particle image velocimetry.

For evaluation the digital PIV recording is divided in small subareas called “interrogation areas”. The local displacement vector for the images of the tracer particles of the first and second

illumination is determined for each interrogation area by means of statistical methods (auto- and cross-correlation). It is assumed that all particles within one interrogation area have moved homogeneously between the two illuminations. The projection of the vector of the local flow velocity into the plane of the light sheet (two-component velocity vector) is calculated taking into account the time delay between the two illuminations and the magnification at imaging.
The process of interrogation is repeated for all interrogation areas of the PIV recording. With modern charge coupled device (CCD) cameras (1000×1000 sensor elements and more) it is possible to capture more than 100 PIV recordings per minute. High-speed recording on complementary metal-oxide semiconductor (CMOS) sensors even allows for acquisition in the kHz range (Raffel et al., 2007). The evaluation of one digital PIV recording with several thousand instantaneous velocity vectors (depending on the size of the recording, the interrogation area and processing algorithm) is of the order of a second with standard computers. If data is required at even faster rates for online monitoring of the flow, dedicated software algorithms which perform evaluations of reduced precision within fractions of a second are commercially available.

Main features

The main features of PIV indicated by Raffel et al. (2007) as follows:
Non-intrusive velocity measurement. In contrast to techniques for the measurement of flow velocities employing probes such as pressure tubes or hot wires, the PIV technique being an optical technique works non-intrusively. This allows the application of PIV even in high-speed flows with shocks or in boundary layers close to the wall, where the flow may be disturbed by the presence of the probes.
Indirect velocity measurement. In the same way as with laser Doppler velocimetry the PIV technique measures the velocity of a fluid element indirectly by means of the measurement of the velocity of tracer particles within the flow, which – in most applications – have been added to the flow before the experiment starts. In two phase flows, particles are already present in the flow. In such a case it will be possible to measure the velocity of the particles themselves as well as the velocity of the fluid (to be additionally seeded with small tracer particles).
Whole field technique. PIV is a technique which allows to record images of large parts of flow fields in a variety of applications in gaseous and liquid media and to extract the velocity information out of these images. This feature is unique to the PIV technique. Aside from Doppler Global Velocimetry (DGV, also known as "Planar Doppler Velocimetry") (Samimy and Wernet, 2000; Elliot and Beutner, 1999; Meyers and Komine, 1991;, Röhle, 1997), which is a new technique particularly appropriate for medium to high-speed air flows, and Molecular Tagging Velocimetry (MTV) (Koochesfahani M.M., et al. 1997) all other techniques for velocity measurements only allow the measurement of the velocity of the flow at a single point, however in most cases with a high temporal resolution. The spatial resolution of PIV is large, whereas the temporal resolution (frame rate of recording PIV images) is limited due to current technological restrictions. These features must be kept in mind when comparing results obtained by PIV with those obtained with traditional techniques. Instantaneous image capture and high spatial resolution of PIV allow the detection of spatial structures even in unsteady flow fields.
Velocity lag. The need to employ tracer particles for the measurement of the flow velocity requires us to check carefully for each experiment whether the particles will faithfully follow the motion of the fluid elements, at least to that extent required by the objectives of the investigations. Small particles will follow the flow better.
Illumination. For applications in gas flows a high power light source for illumination of the tiny tracer particles is required in order to well expose the photographic film or the video sensor by scattered light. However, the need to utilize larger particles because of their better light scattering efficiency is in contradiction to the demand to have as small particles as possible in order to follow the flow faithfully. In most applications a compromise has to be found. In liquid

flows larger particles can usually be accepted which scatter much more light. Thus, light sources of considerably lower peak power can be used here.

Duration of illumination pulse. The duration of the illumination light pulse must be short enough to "freeze" the motion of the particles during the pulse exposure in order to avoid blurring of the image ("no streaks").

Time delay between illumination pulses. The time delay between the illumination pulses must be long enough to be able to determine the displacement between the images of the tracer particles with sufficient resolution and short enough to avoid particles with an out-of-plane velocity component leaving the light sheet between subsequent illuminations.

Distribution of tracer particles in the flow. At qualitative flow visualization certain areas of the flow are made visible by marking a stream tube in the flow with tracer particles (smoke, dye). According to the location of the seeding device the tracers will be entrained in specific areas of the flow (boundary layers, wakes behind models, etc.). The structure and the temporal evolution of theses structures can be studied by means of qualitative flow visualization. For PIV the situation is different: a homogeneous distribution of medium density is desired for high quality PIV recordings in order to obtain optimal evaluation. No structures of the flow field can be detected on a PIV recording of high quality.

Density of tracer particle images. Qualitatively three different types of image density can be distinguished (Adrian, 1991), which is illustrated in Figure 2. In the case of low image density (Figure 2a), the images of individual particles can be detected and images corresponding to the same particle originating from different illuminations can be identified. Low image density requires tracking methods for evaluation. Therefore, this situation is referred to as "Particle Tracking Velocimetry", abbreviated "PTV". In the case of medium image density (Figure 2b), the images of individual particles can be detected as well.

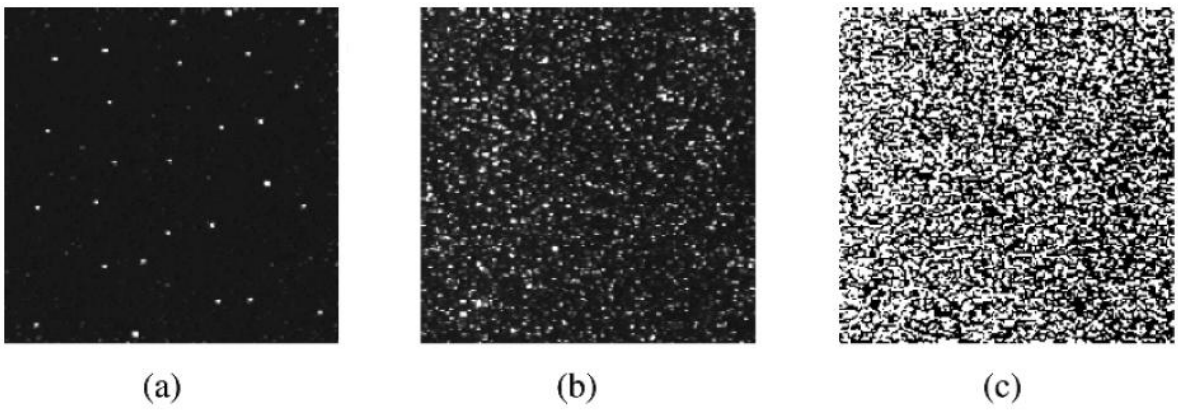

Figure 2: The three modes of particle image density: (a) low (PTV), (b) medium (PIV), and (c) high image density (LSV).

However, it is no longer possible to identify image pairs by visual inspection of the recording. Medium image density is required to apply the standard statistical PIV evaluation techniques. In the case of high image density (Figure 2c), it is not even possible to detect individual images as they overlap in most cases and form speckles. This situation is called "Laser Speckle Velocimetry" (LSV), a term which has been used at the beginning of the nineteen-eighties for the medium image density case as well, as the (optical) evaluation techniques were quite similar for both situations.

Number of illuminations per recording. For both photographic and digital techniques, we have to distinguish whether it is possible to store images of the tracer particles on different frames for each illumination or whether all particle images due to the different illuminations are stored on a single frame.

Number of components of the velocity vector. Due to the planar illumination of the flow field only two (in plane) components of the velocity vector can be determined in standard two-component PIV (2C-PIV). Methods are available to extract the third component of the velocity vector as well (stereo techniques, dual-plane PIV and holographic recording (Hinsch, 1995 and 2002), which itself is three-dimensional). This would be labeled 3C-PIV (see Figure 3). Both methods work in planar domains of the flow field (2D-PIV).

Extension of the observation volume In the most general way an extension of the observation volume is possible by means of holographic techniques (3D-PIV) (Royer and Stanislas, 1996). Other methods such as establishing several parallel light sheets in a volume (Hinsch, 1995) or scanning a volume in a temporal sequence (Brücker, 1996a and 1996b) would be referred to as 2+1D-PIV.

Temporal resolution. Most PIV systems allow to record with high spatial resolution, but at relative low frame rates. However, the recent development of high-speed lasers and cameras allows time resolved measurements of most liquid and low-speed aerodynamic flows.

Spatial resolution. The size of the interrogation areas during evaluation must be small enough for the velocity gradients not to have significant influence on the results. Furthermore, it determines the number of independent velocity vectors and therefore the maximum spatial resolution of the velocity map which can be obtained at a given spatial resolution of the sensor employed for recording.

Repeatability of evaluation. In PIV full information about the flow velocity field (except the time delay between pulses and magnification at imaging) is stored at recording time at a very early stage of data reduction. This results in the interesting feature that PIV recordings can easily be exchanged for evaluation and post-processing with others employing different techniques. The information about the flow velocity field completely contained in the PIV recording can be exploited later on in quite a different way from that for which it had originally been planned without the need to repeat the experiment. In this section the main features of the PIV technique have been described briefly to support a general understanding of its unique features. PIV offers new insights in fluid mechanics especially in unsteady flows as it allows for capturing the whole velocity fields instantaneously. However, other quantitative flow visualization techniques (Merzkirch, 1987) giving information about other important physical quantities of a fluid such as density, temperature, concentration, etc., are already well known and widely used, and new optical methods for the measurement of quantities on the surface of a model such as pressure or deformation are developed. Hence, a more complete experimental description of a complex flow field will be possible and available for comparison with the results of numerical calculations in future by combination of different techniques.

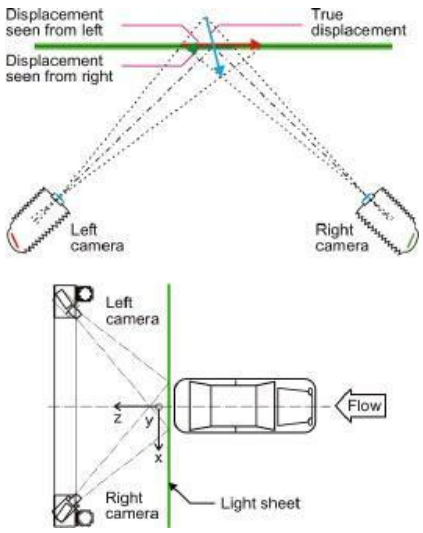

Figure 3: Experimental setup for stereoscopic PIV measurements of the flow behind a car model.

Basic elements

Seeding

Seeding the flow with light reflecting particles is necessary in order to image the flow field. The particles should be small enough to follow the flow but large enough to reflect the required amount of light. In general one can say that PIV needs a higher seeding density than LDV (Laser Doppler Velocimetry). A good rule of thumb is that around ten particles should be correlated for each measured velocity vector.

A good review paper on tracer particles and seeding for PIV systems is found in Melling (1997). This paper discusses about, the specifications for PIV seeding particles with respect to light scattering characteristics; the aerodynamic tracking capability; a review of the types of particle used in various PIV applications and methods of generating and seeding suitable particles.

Descriptions of seeding particles and their characteristics have been given in many scientific publications. In contrast to that, little information can be found in the literature on how to practically supply the particles into the flow under investigation. Sometimes seeding can be done very easily or does not even have to be done. The use of natural seeding is sometimes acceptable, if enough visible particles are naturally present to act as tracers for PIV. In almost all other work it is desirable to add tracers in order to achieve sufficient image contrast and to control particle size. For most liquid flows, seeding can easily be done by suspending solid particles into the fluid and mixing them in order to ensure a homogeneous distribution.

A number of different particles which can be used for flow visualization, LDV and PIV, are listed in Table 1 for liquid and in Table 2 for gas flows (Raffel et al., 2007).

Table 1: Seeding materials for liquid flows.

Type	Material	Mean diameter in μm
Solid	Polystyrene	10 – 100
	Aluminum flakes	2 – 7
	Hollow glass spheres	10 – 100
	Granules for synthetic coatings	10 – 500
Liquid	Different oils	50 – 500
Gaseous	Oxygen bubbles	50 – 1000

Table2: Seeding materials for gas flows.

Type	Material	Mean diameter in μm
Solid	Polystyrene	0.5 – 10
	Alumina Al_2O_3	0.2 – 5
	Titania TiO_2	0.1 – 5
	Glass micro-spheres	0.2 – 3
	Glass micro-balloons	30 – 100
	Granules for synthetic coatings	10 – 50
	Dioctylphathalate	1 – 10
	Smoke	< 1
Liquid	Different oils	0.5 – 10
	Di-ethyl-hexyl-sebacate (DEHS)	0.5 – 1.5
	Helium-filled soap bubbles	1000 – 3000

In gas flows, the increased difference in density between the gaseous bulk fluid and the particles can result in a significant velocity lag. Health considerations are also more important since the experimentalists may inhale seeded air, for example in wind tunnels with an open test section.

The particles which are often used are not easy to handle because many liquid droplets tend to evaporate rather quickly. Solid particles are difficult to disperse and tend to agglomerate. Very often the particles must be injected into the flow shortly before the gaseous medium enters the test section. The injection has to be done without significantly disturbing the flow, but in a way and at a location that ensures homogeneous distribution of the tracers. Since the existing turbulence in many test setups is not strong enough to mix the fluid and particles sufficiently, the particles have to be supplied from a large number of openings. Distributors, like rakes consisting of many small pipes with a large number of tiny holes, are often used. Therefore, particles which can be transported inside small pipes are required.
A number of techniques are used to generate and supply particles for seeding gas flows (Hunter and Nichols, 1985; ; Kähler, 2002, and 2003; Melling, 1986 and 1997; Meyers, 1991). Dry powders can be dispersed in fluidized beds or by air jets. Liquids can be evaporated and afterwards precipitated in condensation generators, or liquid droplets can directly be generated in atomizers. Atomizers can also be used to disperse solid particles suspended in evaporating liquids (Wernet and Wernet, 1994), or to generate tiny droplets of high vapor pressure liquids (e.g. oil) that have been mixed with low vapor pressure liquids (e.g. alcohol) which evaporate prior to entry in the test section. For seeding wind tunnel flows condensation generators, smoke generators and monodisperse polystyrene or latex particles injected with water-ethanol are most often used for flow visualization and LDV.

Light Sources

Lasers are widely used in PIV, because of their ability to emit monochromatic light with high energy density, which can easily be bundled into thin light sheets for illuminating and recording the tracer particles without chromatic aberrations.
PIV can be accomplished using continuous wave (CW) lasers or, more optimally, pulsed lasers. Typical CW lasers used for PIV are argon-ion lasers producing in the range of a few watts; for some less demanding applications, even low-powered helium-neon lasers might suffice. Typical pulsed lasers are frequency-doubled Nd : YAG (neodymium : yttrium aluminum garnet) lasers producing 0.1 to 0.3 joules/pulse, at a repetition rate of tens of Hz (see Figure 4).
Pulses can be created from a CW laser using a chopper, or by rapidly sweeping the entire laser beam through the test-section by reflecting it off a rotating polygonal mirror with all but two facets covered . In the case of the chopped beam, a light sheet must still be created using a sheet-forming module. In the case of the swept-beam, a sheet-forming module is unnecessary because the sweeping action of the beam creates the 'sheet'; although the light sheet is not an instantaneous entity, it constitutes an adequate substitute if the beam is swept rapidly when compared to the unsteadiness of the flow.
The advantage of pulsed lasers is the short duration of the laser pulse, typically a few to several nanoseconds. As a consequence, a particle travelling at even very high speeds is essentially 'frozen' during the exposure with minimal blurring (for example, a particle travelling at 100 m/s will move only 0.06 mm during a 6 nanosecond pulse). Pulsed lasers operate by discharging energy stored in capacitor banks at discrete time intervals to the flash-lamp followed by the laser pulse. Pulsed lasers are ideally suited for PIV because they store and deliver all of the laser power at exactly the desired instant. Pulsed lasers for PIV operate at a constant repetition rate of a few tens of Hz. Therefore, in order to obtain arbitrary Δt's,, one requires two identical lasers firing in tandem. As shown in Figure 5 (Prasad, 2000), the pulse train from the second laser can be produce arbitrarily small Δt's. A delay box producing the required trigger signals must be incorporated to ensure that the lasers, camera, computer, and other hardware are synchronized. With suitable hardware, one can obtain cinematic PIV data with a frame-rate equal to the repetition rate of the lasers. Of course, when working with two lasers, extreme care must be exercised to ensure that the two laser sheets exactly overlap inside the test-section. A lack of such overlap can lead to poor correlation and unsatisfactory results.

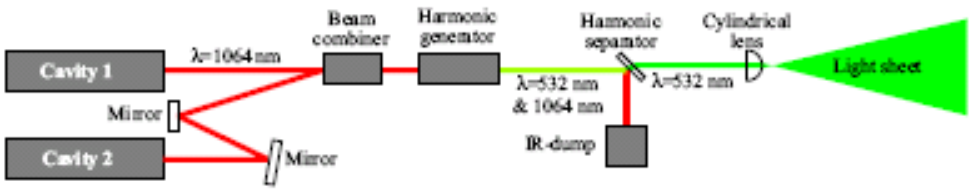

Figure 4: Double cavity Nd:YAG PIV-laser (Törnblom, 2004).

In contrast, CW lasers deliver energy on a continuous basis and 'pulsing' is obtained by either chopping or sweeping the beam. In the case of a chopped laser beam, the light energy incident on a particle increases with the duration of the pulse so created. However, if the pulse duration is too long the particle will produce streaks rather than crisp circular images. (To a small extent, streaky images can be tolerated in correlation-based PIV.)
In general, the amount of CW laser energy incident upon a particle decreases as the flow velocity increases, which places an upper bound on the flow velocity. In contrast, in the case of pulsed lasers, the quality of particle images is immune to the flow velocity. While pulsed lasers are optimally suited for PIV, many fluid mechanics laboratories may already possess argon–ion lasers which could be implemented in a low cost illumination system for low-speed flows.

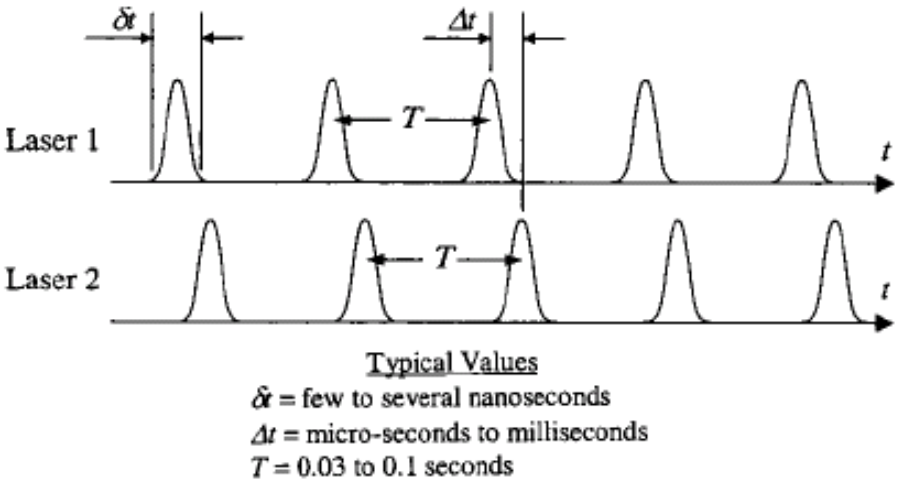

Figure 5: Staggered pulse trains from twin pulsed lasers for PIV

A more detail discussion on different types of lasers used in PIV and various lens configurations for producing thin light sheet is found in Raffel et al. (2007).
Whereas most conventional PIV investigations utilize light sheet illumination, they are typically not a practical source of illumination for micro-flows, due to a lack of optical access along with significant diffraction in light sheet forming optics. Consequently, the flow must be volume illuminated, leaving two choices for the visualization of the seed particles – with an optical system whose depth of field exceeds the depth of the flow being measured or with an optical system whose depth of field is small compared to that of the flow. Both of these techniques have been used in various implementations of μPIV. Cummings (2001) uses a large depth of field imaging system to explore electro-kinetic and pressure-driven flows. Figure 6 shows volume illumination for an imaging system whose depth of field is smaller than that of the flow domain. The optical system will then sharply focus those particles that are within the depth of field δz_m of the imaging system while the remaining particles will be unfocused – to greater or lesser degrees – and contribute to the background noise level.

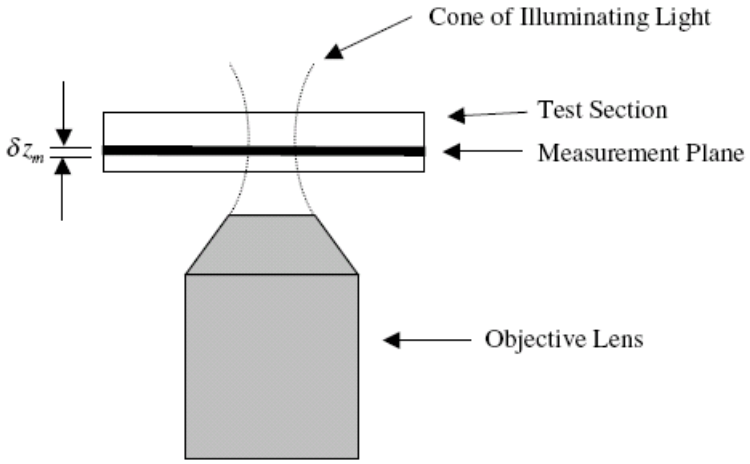

Figure 6: Schematic showing the geometry for volume illumination particle image velocimetry. The particles carried by the flow are illuminated by light coming out of the objective lens (i.e. upward).

This mode of illumination (see also Meinhart et al., 2000) has been used to measure three-dimensional velocity vectors using a single camera (Willert and Gharib,1992), multiple cameras (Okamoto et al., 1995) and a holographic camera (Gray and Greated,1993; Hinsch, 1995). Volume illumination is also advantageous when one is interested in measuring flows through micro electromechanical systems (MEMS) for which optical access is limited to one direction and the length scale is of the order of micrometres (Meinhart and Zhang, 2000).

Image capturing

The PIV recording modes can be classified into two main categories: (1) methods which capture the illuminated flow on to a single frame and (2) methods which provide a single illuminated image for each illumination pulse. These branches are referred to as "single frame/multi-exposure PIV" and "multi-frame/single exposure PIV" respectively (Adrian, 1991).

The principal distinction between the two categories is that the former method, without additional effort, does not retain information on their temporal order of the illumination pulse giving rise to a directional ambiguity in the recovered displacement vector. This necessitated the introduction of a wide variety of schemes to account for the directional ambiguity, such as displacement biasing, the so-called image shifting (i.e. using a rotating mirror or birefringent crystal), pulse tagging or color coding (Hinsch et al., 1987; Adrian, 1986; Goss et al., 1989; Grant and Liu, 1990; Landreth, 1988; Landreth and Adrian, 1988).

In contrast, multi-frame/single exposure PIV recording inherently preserves the temporal order of the particle images and hence is the method of choice if the technological requirements can be met. Also in terms of evaluation this approach is much easier to handle.

Historically single frame/multi-exposure PIV recording was first utilized in conjunction with photography (Raffel et al, 2007). Although multiple frame/single exposure PIV recording is possible using high-speed motion cameras, other problems such as interframe registration arise. Continual development over the past decade in the area of electronic imaging has made multi-frame/single exposure PIV recording possible at flow velocities extending into the hypersonic domain. Depending on the choice of priority an appropriate system for recording can be configured. However, it must be kept in mind that not every requirement can be fulfilled, which is mainly due to technical limitations such as the available laser power, pulse repetition rates, camera frame rate, etc. The selection of the recording system also influences the method for directional ambiguity removal and, hence, the evaluation technique to be used. Today, photographic recording and mechanical image shifting – which have been used for a long time because of the obtained quality of the recordings – might not be considered the first choice anymore. Video recording offers so many advantages by allowing for immediate feedback and

quality optimization during the course of the experiment. This is of high interest for most applications, especially with a view to operational costs.

A number of important photographic parameters need (as pinpointed by Grant, 1997) to be considered when estimating the dynamic range of a flow measuring system based on the PIV method. These are as below:

1. The spatial resolution of an image capture system is determined by the vertex angle (α) of the cone of light (determined by the camera aperture $f^{\#)}$ and the illuminating light wavelength λ. Ignoring constant multiplicative factors, the transverse resolution is given by the Rayleigh criterion as $d_1 \approx \lambda/\alpha$ and the longitudinal resolution as $d_2 \approx \lambda\alpha^2$. For instance, at unit magnification, an $f^{\#}$ 2.8 lens gives a 6λ transverse resolution and a 30λ longitudinal resolution (Born and Wolf, (1970).

2. Depth of field. In order to obtain a sharp image the object particle needs to fall within the depth of field of the camera lens. This is the region in which the image is 'acceptably' sharp. The limits on image sharpness can be related to the diameter of the circle of confusion, the diameter of the disc in the image plane representing a point in the object plane. The depth of field (DOF) may be written as $2F(1+M)^2 f^{\#}/10^6 M$ to a good approximation (Marrett, 1967). Alternatively, $DOF=4(1+1/M)^2 f^{\#2} \lambda$ (Offutt, 1995). In principle, the use of a narrow-width laser sheet image dent with the in-focus plane may be used to ensure density in-focus images. For example, if the particles are small and high spatial resolution is required $f^{\#}=8$ and λ= 0.6993mm may be taken, giving a depth of field of 0.7mm. If a larger depth of field is required then the $f^{\#}$ must be increased with a resulting loss in resolution.

3. Image size. If the particle image can be resolved, its size will depend on the particle diameter, d_p the lens magnification, M, and the point response function (PRF) of the lens. If the particle falls within the depth of field of the lens the geometrical image diameter is given by $d_{GI} = Md_p$. When the lens is diffraction limited the PRF is an Airy function of diameter $d_A = 2.44\ (1+M)f^{\#}$. The image is obtained by convoluting the PRF with the geometrical image of the par ticle. An estimate of this effect can be obtained by replacing both the Airy function and the particle image by Gaussian functions, leading to the approximation for the image diameter $d_1 = M^2 d^2_{GI} + d^2_A$ (Adrian and Yao, 1985).

Typically, in a PIV experiment M=1, $f^{\#}=8$ and λ=0.6993μm. In this case d_A=25μm so d_1 is effectively independent of particle size for particles less than 10μm in diameter. When d_P>50μm then the image size is effectively the geometrical particle image size.

4. Recording medium. The recording medium chosen is dependent on the size of flow field to be recorded and the required resolution. For example, a CCD (charge coupled device) (digital) camera of 512×512 pixels (digital picture elements) represents the image by 2.6×10^5 pixels whereas a large format photographic transparency (100 mm×125 mm) of 300 lines/mm of film contains the equivalent of 1.1×10^9 pixels. Higher resolution CCD cameras are now available using a 2048×2048 format (or higher in specialist cameras). This means that single-image files may contain 42×10^5 pixels. This has implications for speed in the data handling and storage by the host computer. The CCD camera captures data at the video framing rate of 25 frames/s, with the digital image data being passed to a frame board storage, on-board processing and forwarding to digital memory.

Recording hardware

Recent advances in electronic imaging have forced the photographic methods mostly aside. Immediate image availability and thus feedback during recording as well as a complete avoidance of photochemical processing are a few of the apparent advantages brought about with electronic imaging. The present trends suggest that electronic recording will even be able to substitute large format film cameras and holographic plates in near future. For this reason more attention is placed on the description of electronic recording although it should be noted that the development in this area is very rapid.

There is a variety of electronic image sensors available today, but majorly solid state sensors are used. Although electronic imaging based on vidicon tubes has reached a high state of

development since their introduction more than 50 years ago, their importance to typical imaging applications has decreased dramatically in favor of solid state sensors.
The most common are charge coupled devices, or CCD, charge injection devices (CID) and complementary metaloxide semiconductor (CMOS) devices. Over the past two decades, the CCD has found the most widespread use. However, the rapid development of chip technology in the early 90s of the last century allowed the manufacturing of CMOS sensors with an improved signal-to-noise ratio and resolution. Since a couple of years they are more and more frequently used for digital photography, machine vision and, last but not least, for high-speed PIV (Raffel et al., 2007).
PIV images is usually recorded on a film or on CCD sensors. The popular trend nowadays is to use CCD cameras for PIV recordings. However, photographic film may still be a viable choice when very high resolutions are required.
PIV puts special demands on the camera that is going to be used, especially if the flow velocity is high, the imaged area is small and if the particles are small. The first two circumstances requires the camera to be able to take two images within a short period of time in order for the same individual particles to appear in both images. Short inter exposure times can be achieved either by having a high speed camera which continuously records images at a rate of several kHz or by using a camera with a progressive scan architecture. With a high speed camera the shortest inter image time possible today is around 10 μs and this is achieved by letting the first laser pulse come at the end of the exposure of the first image and the second pulse in the beginning of the exposure of the second image, c.f. Figure 7 (Törnblom, 2004). Cameras with progressive scan architecture can take two images with less than 1 μs delay. Directly after the first image has been recorded the charge of each pixel is transferred to its designated position in the interline shift register, a new image can now be recorded by the pixels. The second image is exposed until the first image has been read out from the interline shift register and is then transferred to the image buffer in the same way. The second image will due to this procedure be exposed for a longer time than the first and to avoid it becoming overexposed by ambient light a filter which only pass the laser wavelength can be fitted on the camera lens.

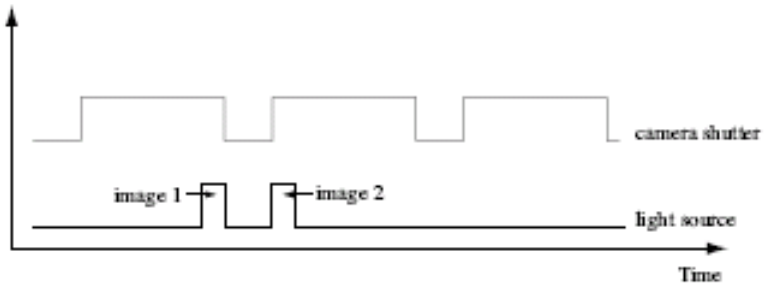

Figure 7: How short inter image times are achieved when using continuous high speed cameras.

If the particles are small or if the light intensity is low the camera needs to have a high sensitivity to incoming light. The sensitivity of a photon sensor such as a CCD-camera is measured in QE (quantum efficiency) which is the average number of electrons that are released from the sensor when it is hit by a photon. The QE is often wavelength dependent with a maximum efficiency in the blue-green part of the visible spectrum. The most sensitive cameras have a QE of around 70%. Since the laser light is monochromatic there is no need to use a colour camera, this also makes the image files smaller.

Image processing

In order to extract the displacement information from a PIV recording some sort of interrogation scheme is required. Initially, this interrogation was performed manually on selected images with relatively sparse seeding which allowed the tracking of individual particles (Agüi and Jiménez,

1987; Dracos, 1996). With computers and image processing becoming more commonplace in the laboratory environment it became possible to automate the interrogation process of the particle track images (Grant and Liu, 1989; Gharib and, Willert, 1990; Guezennec et al., 1994; Virant and Dracos 1996). However, the application of tracking methods, that is to follow the images of an individual tracer particle from exposure to exposure, is only practicable in the low image density case, see Figure 2(a). The low image density case often appears in strongly three-dimensional high-speed flows (e.g. turbomachinery) where it is not possible to provide enough tracer particles or in two phase flows, where the transport of the particles themselves is investigated. Additionally, the Lagrangian motion of a fluid element can be determined by applying tracking methods [Cenedese and Querzoli, 1995; Siu et al., 1994; Dracos, 1996). In principle, however, a high data density is required on the PIV vector maps, especially for the comparison of experimental data with the results of numerical calculations. This demand requires a medium concentration of the images of the tracer particles in the PIV recording. (In particular, in air flows it is not possible to achieve a high image density, because beyond a certain level the number of detectable images cannot be increased by further increasing the tracers density in the flow (Adrian and Yao, 1985).) Medium image concentration is characterized by the fact that matching pairs of particle images – due to subsequent illuminations – cannot be detected by visual inspection of the PIV recording, see Figure 2(b). Hence statistical approaches had to be developed. After a statistical evaluation has been performed first, tracking algorithms can be applied additionally in order to achieve sub-window spatial resolution of the measurement, which is known as "super resolution" PIV (Keane et al., 1995). However, since the extraction of the displacement information from individual particle images requires spatially well resolved recordings of the particle images, those techniques are more appropriate to increase the spatial resolution of photographic PIV recordings than that of digital recordings (Raffel et al., 2007).

Tracking algorithms have continuously been improved during the past decade. Methods like the application of neural networks (Grant and Pan, 1995; Carasone et al., 1995) seem to be very promising. Thus, for some applications particle tracking might be an interesting alternative to statistical PIV evaluation methods. Readers interested in obtaining a survey of tracking methods are referred to the references (Grant, 1997; Dracos, 1996; Grant, 1994).

A comparison between cross-correlation methods and particle tracking techniques together with an assessment of their performance has recently been performed in the framework of the "International PIV Challenge" (Stanislas et al., 2003; Stanislas et al., 2005).

Basically three advanced methods have been applied to the problem of extracting displacement information from a PIV record (Buchhave, 1992): (1) evaluation of the fringe spacing and direction of the so-called Youngs' fringes [the spatial power spectrum (PS) of the PIV image], (2) direct two-dimensional autocorrelation (ACF) of the PIV image, and (3) a probability analysis of the displacement information in the PIV image (Takai and Asakura, 1988; Humphreys, 1991). As described by Adrian (1988), the optimum analysis of the Young's fringe pattern to find the spacing and direction of the fringes is a two-dimensional Fourier transform (F'F), which makes the two first mentioned methods essentially equivalent. If the image information is recorded in two separate pictures, one for the first illumination and another for the second illumination, a cross-correlation (CCF) can be applied to find the displacement without directional ambiguity.

The correlation procedures can be carried out on a digital computer. A general scheme for this task is depicted in Figure 8. The PIV image (transparency) is illuminated by a light source. This may be a white light source or a laser source; the important thing is to have enough light to be able to image the interrogation area onto an image-resolving electronic detector (eg, a CCD camera). As the IA is recorded and processed, the film is scanned to the next IA, resulting in a pointwise interrogation of the whole image.

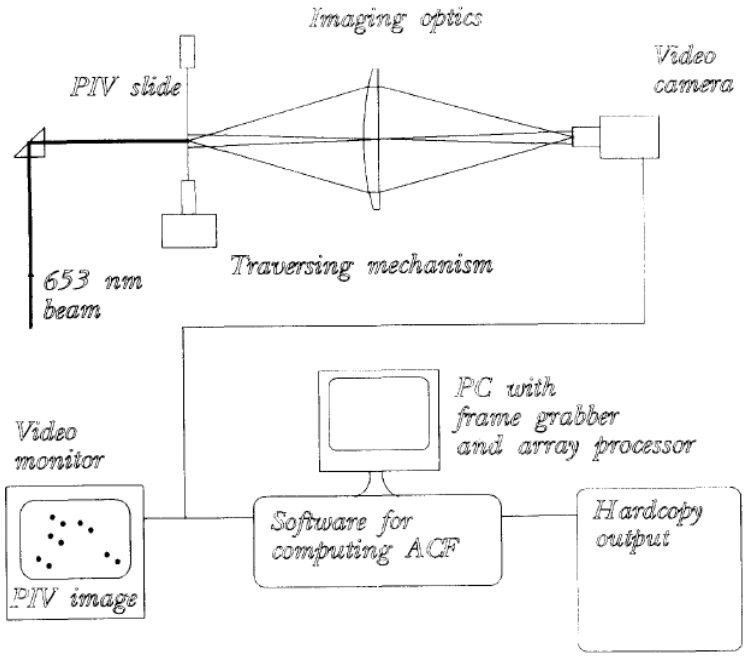

Figure 8: Hardware for digital ACF of PIV image.

The detector signal is digitized and stored in the computer memory or on a nonvolatile medium. The usual procedure is to apply a so-called framegrabber, which is an electronic device now available in the form of a plug-in board for a personal computer. The framegrabber is able to digitize one video flame from the detector and transfer the digitized information to a video memory area located on the board.

The signal processing procedure consists of a standard digital auto- or cross-correlation on the stored image. The standard procedure is to apply a two-dimensional fast Fourier transform (FFT) routine followed by a squaring of the image data to obtain the PS followed by a second FFT to obtain the ACF. Although these operations are standard and were developed for high speed on a digital computer, the processing of one IA may take several seconds even on a fast, dedicated processor, and even using the largest systems normally available for this type of experiments the processing of one IA may take about 0.5-1s (Landreth and Adrian, 1988). An optical technique for reducing a two-dimensional PIV image array to two one-dimensional arrays has been proposed by Yao and Adrian (Yao and Adrian, 1984). This technique would speed up the reading and signal processing of the PIV image by avoiding the two-dimensional FFT transform, but the compression technique results in a reduction of the signal-to-noise ratio because all the background noise is integrated into the one-dimensional arrays. A similar orthogonal projection method performed on the digitized image has been proposed by Cenedese and Paglialunga (1987). The advantages of using cross-correlation analysis have been summarized by Cho (1989), who investigates the possibility of removing the diffraction halo function (the single-exposure diffraction pattern in the Young's fringe plane) and determining the flow direction. Some alternative digital ACF and PS estimators have also been investigated [Cenedese and Paglialunga, 1990).

Optical methods can be used to speed the data processing of PIV images. It is straightforward to try to apply the Fourier transforming properties of a lens to the data processing of PIV images. This is often referred to as Young's fringe analysis. The resolution of an optical Fourier transform is of the same order as the resolution of state-of-the-art framegrabbers and also matches the accuracy inherent in the PIV image. Thus a good balance between hardware and measurement accuracy is expected. A combined optical/digital processor based on these principles is shown in figure 7 of Buchhave (1992).

Advanced techniques

Digital particle image velocimetry

Digital particle image velocimetry (DPIV) is the digital counterpart of conventional laser speckle velocitmetry (LSV) and particle image velocimetry techniques. In this novel, two-dimensional technique, digitally recorded video images are analyzed computationally, removing both the photographic and opto-mechanical processing steps inherent to PIV and LSV. The directional ambiguity generally associated with PIV and LSV is resolved by implementing local spatial cross-correlations between two sequential single-exposed particle images. High resolution video systems with higher framing rates become more economically feasible. Sequential imaging makes it possible to study unsteady phenomena like the temporal evolution of a vortex ring (Willert and Gharib, 1991).

The development of digital cameras of medium (512×512 pixels) to high (2048×2048 pixels and beyond) format has encouraged the development of DPIV (Grant, 1997). The acquisition of PIV images in digital form eliminates the photographic stage and makes multiframe and ensemble measurements easier. The disadvantages of using DPIV are the data rates (defined by the video framing rate of 25 Hz) and the loss of spatial resolution (Willert and Gharib, 1991; Merzkirch et al., 1994).

In DPIV the combination of multiple pulsing and multiple framing can be used to increase the dynamic range (Lim et al., 1994). Frame-by-frame flow tracer cross-correlation has been applied to video images (Kimura and Takamori, 1986). The equations associated with the digital equivalent of Young's fringes have been formulated and investigated by numerical simulation (Cho, 1989). Numerous DPIV investigations using correlation analysis methods and tracking algorithms in engineering flows have been reported (Westerweel and Nieuwstadt, 1991; Okada et al., 1990; Westerwell and Niewestadt, 1990). DPIV has also found useful application in transonic flows (Brystan-Cross et al., 1995).

In DPIV two sequential digital images are sub-sampled at one particular area via an interrogation window (Figure 9). Within these image samples an average spatial shift of particles may be observed from one sample to its counterpart in the other image, provided a flow is present in the illuminated plane. This spatial shift may be described quite simply with a linear digital signal processing model shown in Figure 10. One of the sampled regions f(m, n) may be considered the input to a system whose output g(m,n) corresponds to the sampled region of another image taken a time Δt later. The system itself consists of two components, a spatial displacement function s(m,n) (also known as the system's impulse response) and an additive noise process d(m, n). This noise process is a direct result of particles moving off the edges of the sampling region, particles disappearing through three-dimensional motions in the laser sheet, and the total number of particles present in the window. Of course the original samples f (m, n) and g (m, n) may be noisy as well.

The major task in DPIV is the estimation of the spatial shifting function s (m, n) but the presence of noise d (m, n) complicates the matters (for more detail refer Willert and Gharib, 1991).

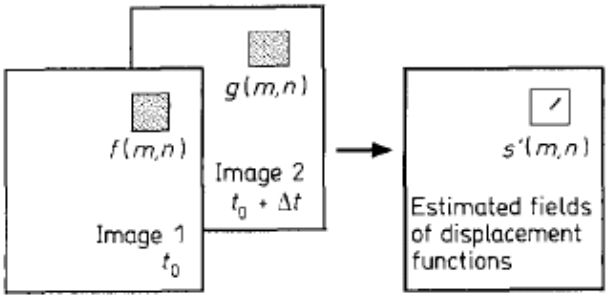

Figure 9: Conceptual arrangement of frame-to-frame subsampling associated with digital particle image velocimetry.

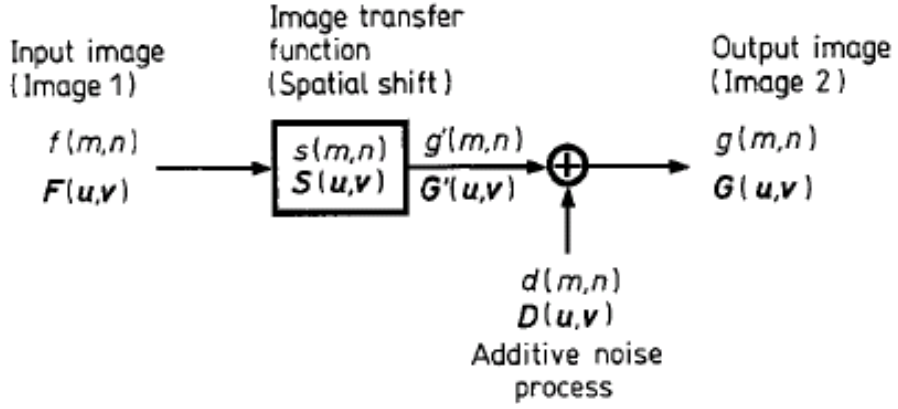

Figure 10: Digital signal processing model describing the functional relationship of two successive frames of displaced particles; capitalized functions are the Fourier transforms of the functions in lower case and represent the spatial frequency domain.

An ultra-high-speed video system has been developed for fast process monitoring (Stasicki and Meier, 1994) and exploited for flow measurement (Raffel et al., 1995). The system allows exposure times down to 0.6 μs and exposure intervals of 50 ns. The system is capable of delivering up to eight frames. The camera uses a beam-splitter mirror and eight framegrabber cards. The capture of the time series of images is controlled by the sequential release of freely triggerable electronic shutters.
The DPIV velocity field computation speed can be increased by two orders of magnitude using a video motion estimation processor (MEP) chip (Roth et al., 1995). The method of computation differs from the correlation approach in that, instead of summing the product of the image intensities, the MEP sums the absolute value of their difference (Grant, 1997).

Stereoscopic (3-component) PIV

In spite of all its advantages, the PIV method contains some shortcomings that necessitate further developments on the basis of instrumentation. One of these disadvantages is the fact that the "classical" PIV method is only capable of recording the projection of the velocity vector into the plane of the light sheet; the out-of-plane velocity component is lost while the in-plane components are affected by an unrecoverable error due to the perspective transformation. For highly three-dimensional flows this can lead to substantial measurement errors of the local velocity vector. This error increases as the distance to the principal axis of the imaging optics increases. Thus it is often advantageous to select a large viewing distance in comparison to the imaged area to keep the projection error to a minimum. This is easily achieved using long focal length lenses. Nevertheless, an increasing number of PIV applications require the additional knowledge of the out-of-plane velocity component.
A variety of approaches capable of recovering the complete set of velocity components have been described in the literature (Hinsch, 1995; Royer and Stanislas, 1996). The most straightforward, but not necessarily easily implemented, method is an additional PIV recording from a different viewing direction using a second camera (Figure 11), which can be generally referred to as stereoscopic PIV recording (Gaydon, 1997; Prasad and Adrian, 1993; Prasad and Jensen, 1995; van Oord, 1997; Westerweel and Nieuwstadt, 1991; Willert, 1997). Reconstruction of the three-component velocity vector in effect relies on the perspective distortion of a displacement vector viewed from different directions.

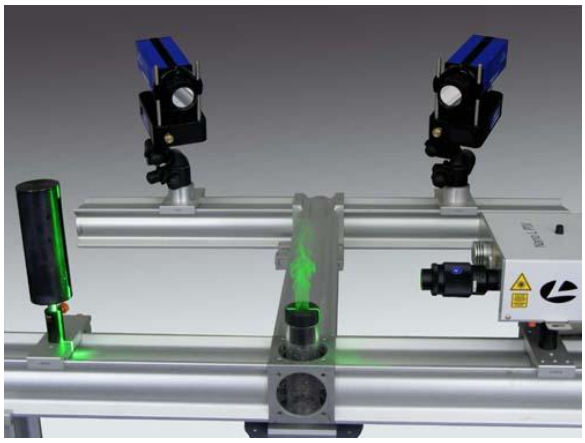

Figure 11: 3D-Stereo PIV is based on the principle of stereoscopic imaging: two cameras capture the image of the illuminated particles from different angles and is well known from the human eyesight.

Two different stereoscopic approaches can be used (Figure 12) (Lourenco and Krothapalli, 1989; Gauthier and Riethmuller, 1988; Willert, 1997). In the angular approach, the optical axes of the two recording cameras are no longer perpendicular to the flow but make a certain angle with the illuminated sheet. In the translational method, the stereoscopic effects are directly related to the distance between the optical axes of the cameras, which are now perpendicular to the illuminated sheet. The main disadvantage of the angular method is that it is not possible to bring the whole of the illuminated plane precisely into focus on the film unless the back of the camera is swung, in which case the recorded images will be affected by distortion. In the translational approach, the common field of view is quite limited due to the axis distance required for sufficient accuracy. Nevertheless, the common field can be easily increased by changing the position of the back of the camera in relation to the lens (Arroyot and Greated, 1991.)
The current trend in stereoscopic PIV seems to favour the use of CCD cameras arranged in angular displacement configuration (Prasad, 2000).

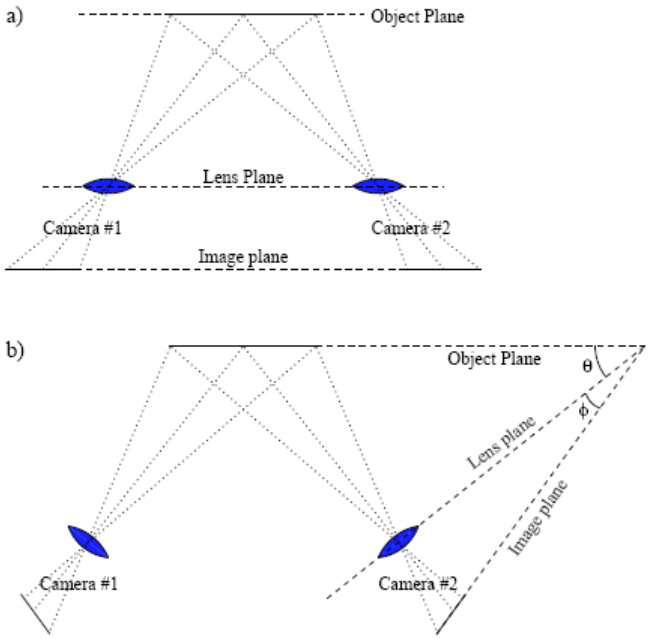

Figure 12: Basic stereoscopic imaging configurations: (a) lens translation method; (b) angular lens displacement with tilted backplane.

Some general recommendation for using stereo PIV as mentioned by Raffel et al. (2007) are:

· Multi-level or translated targets provide sufficiently good calibration results. Volumetric camera calibration commonly found in robot vision is not necessary and generally not possible due to the limited depth of field for large aperture lenses used for PIV.

· Calibration from a single image of a planar target is possible but should only be used if translation is not possible (i.e. due confined space).

· For optimum measurement accuracy the enclosed angle between the camera viewing axes should be close to 90°.

· The unavoidable misalignment between calibration target and light sheet plane requires disparity correction or self-calibration schemes using the actual particle images.

· Disparity correction can also be used to correct for movement of the camera (s) during the measurements (i.e. vibration).

· The minimum PIV sample size should be at least the same size as the light sheet thickness.

· For SPIV experiments in water the air-glass-water interface should be normal to the camera viewing axis to keep the astigmatism minimal. Oblique views are possible by attaching suitable water prisms to the test section (Prasad and Jensen, 1995; van Doorne and Westerweel, 2007).

· Image reconstruction should make use of appropriate image interpolation schemes. For best performance iterative image deformation and image back-projection can be combined in a single step (Wieneke, 2005).

Volumetric PIV measurements

The PIV technique in stereo arrangement as described above has become a standard for the measurement of all three velocity components (3C) in a plane of the flow (2D). This is even true for complex applications in industrial test facilities (e.g. helicopter aerodynamics studies or transonic turbine test rig). In most applications the factor limiting the use of stereo PIV is not associated with PIV equipment or evaluation algorithms but with the limited optical access in such test facilities. This means that the temporal and spatial resolution achievable for stereo (3C) PIV is more or less the same as for 'classical' 2C PIV.

However, there is still no universal method available to capture instantaneous velocity fields in a volume of the flow (3D), in order to be able to investigate complex unsteady 3-dimensional flow phenomena (vortices, boundary layers, separated flows, etc.), which are of increasing importance in both fundamental as well as industrial research. The main reason is that the required laser light sources, cameras, evaluation algorithms, computing capacity, etc. are not yet available today due to lack of technical progress. Thus, different PIV methods need to be applied today depending on the respective application. Holographic PIV methods (HPIV) are in principle suited to capture flow velocity fields completely three-dimensional. The registration of the particle images on high resolution photographic material (photochemical holographic PIV (P-HPIV)) allows a high spatial resolution in a medium sized volume without temporal resolution. Registration via CCD sensors (digital holographic PIV (D-HPIV)) allows time-resolved measurements in a small volume. A new technique (volume PIV or tomographic PIV) achieves the information in depth of the volume via simultaneous observation with several cameras with different viewing angles.

Figure 13 gives an overview of different PIV methods with their spatial and temporal resolution.

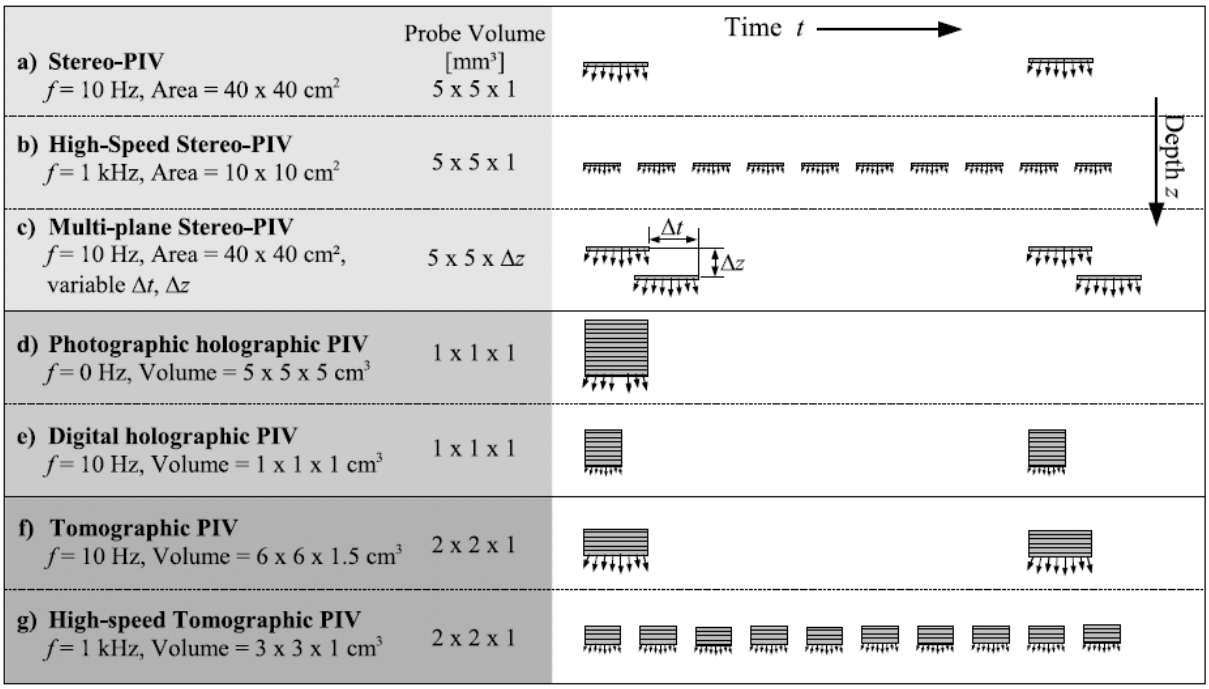

Figure 13: Schematic overview over present variants of the PIV method with their typical spatial and temporal resolution. The symbols present the measurable three-component velocity vectors for each method in their spatial and temporal arrangement (Raffel et al., 2007).

Multiplane stereo PIV

Multi-plane stereo PIV requires several planes of the flow field to be illuminated simultaneously. The particle images within each of such light sheets will be recorded with a separate stereo PIV system. The optical separation of these light sheets will be performed by polarization of different wavelength of the light used for illumination. This method exhibits the same properties as stereo PIV and does not allow to capture a complete volume (see Figure 13c). Information about the instantaneous velocity field being available in different planes, the determination of local velocity gradients and space-time correlation becomes possible. Drawback of this method is the high experimental effort. For each plane a complete stereo PIV system has to be set up together with elements for the required optical separation (polarization, color filters).

The multiplane stereo PIV system, developed for applications in air flows in particular, consists of a four-pulse laser system delivering orthogonally polarized light, two pairs of high resolution progressive scan CCD cameras in an angular imaging configuration with Scheimpflug correction, two high reflectivity mirrors and a pair of polarizing beam-splitter cubes according to Figure 14.

After the illumination of the tracer particles with orthogonally linearly polarized light, the polarizing beam-splitter cube (7) separates the incident wave-front scattered from the particles into two parts according to the state of polarization. The separation based on polarization works perfectly as long as the radius of the spherical particles is comparable to the wavelength of the laser light (see also (Kähler, et al., 2002; Kähler, 2003) for the generation of appropriate particles) and the observation direction is properly aligned relative to the direction of the polarization vector. In the case that these requirements cannot be fulfilled a frequency based multiplane stereo PIV approach can be applied but in this case the laser system has to be modified to generate the required frequency shift [Mullin and Dahm, 2004).

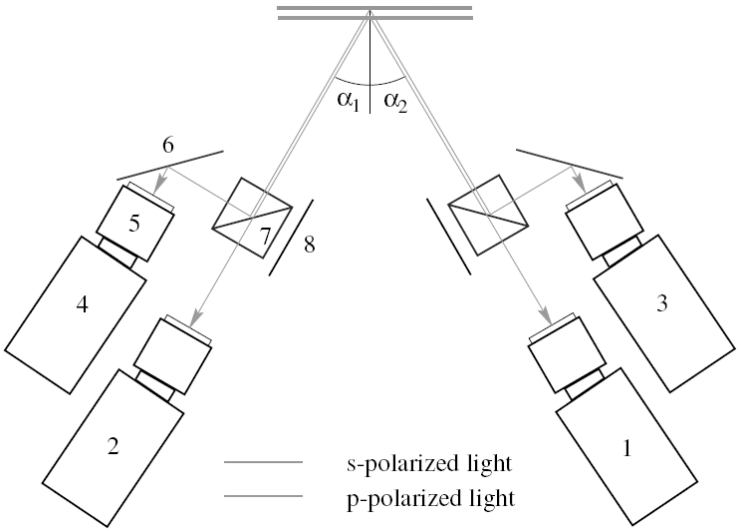

Figure 14: Schematic setup of the recording system. 1-4 digital cameras, 5 lens, 6 mirror, 7 polarizing beam-splitter cube with dielectric coating between the two right-angle prisms, 8 absorbing material, α opening angle (Raffel et al., 2007).

The Multiplane Stereo PIV system is very reliable, robust and well suited for all kinds of applications, purely scientific as well as for industrially motivated investigations in large wind tunnels where acquisition time, optical access and observation distances are constrained. Furthermore, it is based on the conventional PIV equipment and the familiar evaluation procedure so that available PIV systems can easily be expanded. The advantage of this measurement system with respect to other imaging techniques lies in its ability to determine a variety of fundamentally important fluid-mechanical quantities with high accuracy (no perspective error), simply by changing the time sequence or light sheet position. Due to the advantage of this technique relative to conventional PIV systems, it is increasingly applied by other leading research groups all over the world (Braud, 2004; Hu et al., 2001; Mullin and Dahm, 2005).

Holographic PIV

Holography is truly the key to three dimensions in particle image velocimetry, i.e. the measurement of all spatial components of the velocity vector—and this over a deep measuring field. Sophisticated instruments have been designed that successfully tackle practical problems such as the low scattering efficiency of particles, the inferior depth resolution or the aberrations and distortions in the reconstruction. Furthermore, efficient strategies are introduced to interrogate the holographic storage and process the huge amount of data towards a final flow field representation. Recently, phase-sensitive metrology, familiar in many fields of experimental mechanics, has been examined for use in particle velocimetry. Suitable methods are holographic and speckle interferometry or the optical processing of data for three-dimensional correlation. While in these techniques the power of optics is unrivalled, the practical advantage of video and digital techniques over photographic recording is obvious. The electronic version of speckle interferometry (ESPI/DSPI) is a well-established method used in laser metrology and has received further exploitation for applications in flow analysis recently.
Generally, holography is a method used to store the amplitude and phase of a light wave by recording the interference pattern that occurs when a second wave, the so-called reference wave, is superimposed (Hinsch, 2002). The processed interference pattern—a hologram—is used to reconstruct the original wave field by illuminating it with a replica of the reference wave (Collier et al., 1971). There are several methods used to perform such a recording of particles (Royer 2000). Let us illustrate the situation for the so-called off-axis set-up that has become the predominant version used in HPIV. In Figure 15 we meet the familiar arrangement where the

hologram is recorded by superimposing the scattered particle light—the object wave—with a reference wave on a photographic plate. Later, the developed photo (the hologram) is illuminated with the reference wave and diffraction from the pattern of microscopic interference structures reproduces a wave that seems to originate from a particle field—the virtual image.

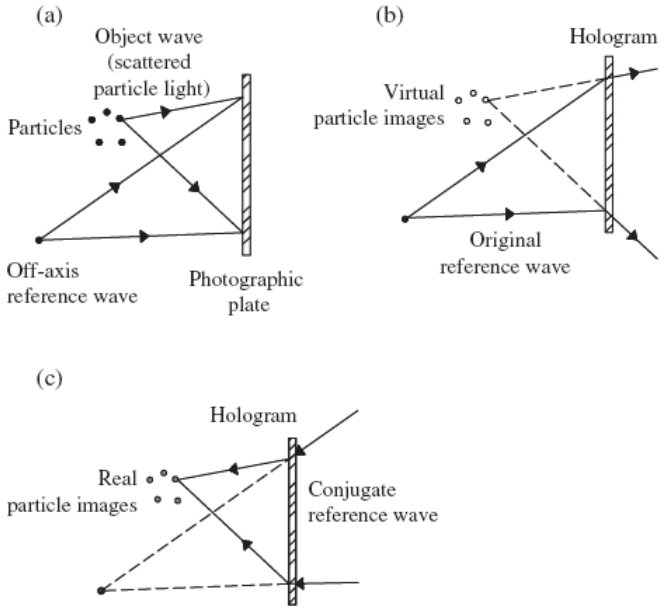

Figure 15: Schematic of optical off-axis set-ups in particle holography. (a) Recording of a hologram of a particle field; (b) reconstruction of a virtual image; (c) reconstruction of a real image (Hinsch, 2002) .

A startling feature of holography is that by reversing the direction of the reconstructing wave—this is called the conjugate reference wave (for a plane wave this is achieved by rotating the plate through 180°)—a real image of the particle field can be produced in space. This lens-less imaging has become the standard configuration in reconstructing particle fields from holograms. Here, the aperture responsible for the accuracy in the particle position is limited only by the area on the hologram that intercepts scattered light from the particles. All efforts connected to large-aperture optics in traditional imaging can be avoided. Real-image reconstruction may also be employed for the successful compensation of aberrations from difficult environments or low-cost relay imaging which is often applied to improve the geometry of the set-up. For this purpose, the aberrating media (like the transparent wall of a circular pipe or an engine head) must be reinserted into the reconstructed object wave (Barnhart et al., 1994).
In classical light-sheet PIV, lasers are preferred because they provide short pulses of high energy. For holography lasers are definitely needed because interference requires coherence. Any light source is characterized by its coherence length, which is the maximum detour path length of two beams that still provides a good interference pattern, i.e. a satisfactory hologram. This value depends on the number of activated axial resonator modes and is related to the spectral width of the fluorescence line of the laser emission and the resonator length. Intra-cavity etalons reduce this number and thus increase the coherence length. In Nd:YAG lasers the coherence length is increased by injection seeding where a high-energy laser is driven by a low-output laser of high coherence. Usually a long coherence length is required in holography to relax restrictions on the depth of the object and the matching of optical paths. Both ruby and Nd:YAG lasers provide coherence of at least a metre. The ultimate limit, of course, is set by the length equivalent to the pulse duration. For special applications such as light-in-flight holography, coherence can be reduced to a few millimetres either by removing etalons or by switching off the seeder. The shortest coherence length is given when all possible modes radiate—the wider the fluorescence line the smaller this value.

This all looks simple. However, there are several basic issues that have influenced all practical realizations and can be encountered throughout the history of HPIV; for earlier overviews see, for example, Rood (1993) and Hinsch (1995). Some of these are tackled by novel methods such as HI, electronic speckle pattern interferometry or optical processing and even digital holography.

Tomographic-PIV

Tomographic-PIV is a measurement technique that allows resolving the particle motion within a three-dimensional measurement volume without the need to detect individual particles. This recently developed method (Elsinga et al., 2006) is based on the simultaneous view of the illuminated particles by digital cameras placed along several observation directions similarly to the stereoscopic PIV configuration. The innovative element of the technique is the tomographic algorithm used to reconstruct the 3D particle field from the individual images. The 3D light intensity distribution is discretized over an array of voxels and then analyzed by means of 3D cross-correlation interrogation returning the instantaneous three-component velocity vector field over the measurement volume.

Tomographic-PIV has been developed for research laboratory applications and its extension to industrial wind tunnel environments so far has not been performed. Despite its recent introduction, by early 2007 the technique has already been successfully applied in both air and water flow measurements within about 10 experiments conducted over several European laboratories (TU Delft, LaVision, DLR G¨ottingen, TU Braunschweig, Poitiers University). The requirement to implement time-resolved Tomographic-PIV is the same as for planar PIV, which has been already verified with both low repetition-rate Tomographic-PIV measurements in water flows and a high-repetition rate boundary layer experiment in air flow.

The most important limiting factors are the extent of the measurement volume depth (typical depth-to-width ratio 0.25), the power required for volume illumination (typically 5 times higher than for a stereo-PIV experiment), the time required for digital evaluation of recordings (nowadays a few hours per snapshot) and the associated data storage (typically 10 times larger than for planar PIV). Last but not least a slightly extended optical access is required with respect to stereo-PIV because the viewing directions typically cover a solid angle, although the linear configuration is also a possible option if required.

Its working principle is that, tracer particles immersed in the flow are illuminated by a pulsed light source within a three-dimensional region of space (Figure 16, Raffel et al., 2007). Particle images are recorded in focus from several viewing directions using CCD cameras. The Scheimpflug condition between the image plane, lens plane and the medianobject- plane has to be fulfilled, which is practically achieved by means of camera-lens tilt mechanisms with the rotation axis freely adjustable. The latter condition is not sufficient to ensure that particle images are in focus over the entire depth of the measurement volume. This requirement is satisfied with an appropriate depth of focus by selecting an appropriate lens aperture.

The reconstruction of the 3D object from the digital images requires prior knowledge of the mapping function between the image planes and the physical space. This is achieved by means of a calibration procedure similar to that of stereoscopic PIV. However the procedure requires such mapping function to be defined onto a volumetric domain as opposed to that used for planarstereo-PIV. The requirement for a precise alignment between calibration and measurement plane is not a restriction in this case since no such plane exists for the tomographic technique, which makes it easier to implement the experiment with respect to laser light positioning. However, the requirement for a precise relative position between cameras for the tomographic technique (one-fifth of the particle image diameter) is much more stringent than that for planar stereo PIV (Raffel et al., 2007).

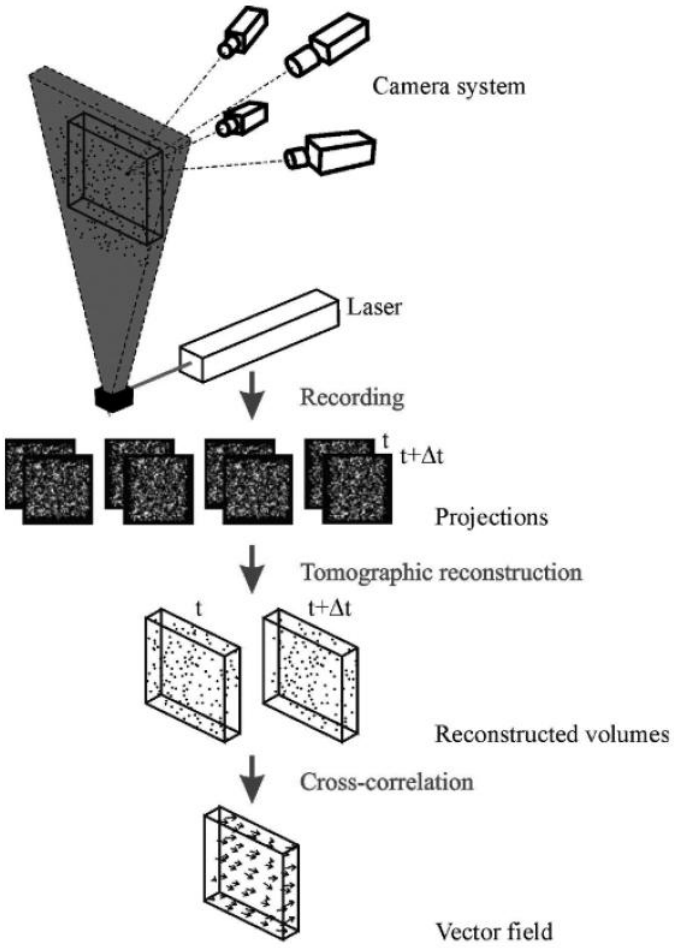

Figure 16: Principle of Tomographic-PIV.

Although recently introduced the tomographic PIV technique has been applied to several flow conditions from more academic configurations such as circular cylinder wakes to increasingly challenging topics such as low speed turbulent boundary layers and shock wave boundary layer interaction at Mach 2. The technique as also been implemented in conjunction with high repetition rate hardware for the time resolved measurement of boundary layer transition to turbulence described in details in the section of PIV applications.

Micro-PIV

Many areas in science and engineering are existing where it is important to determine the flow field at the micron scale. Industrial applications of micro-fabricated fluidic devices are present in the aerospace, computer, automotive, and biomedical industries. In the aerospace industry, for instance, micron-scale supersonic nozzles measuring approximately 35μm are being designed for JPL/NASA to be used as microthrusters on micro-satellites and for AFOSR/DARPA as flow control devices for palm-size micro-aircraft (Bayt and Breuer, 2001). In the computer industry, inkjet printers, which consist of an array of nozzles with exit orifices on the order of tens of microns in diameter, account for 65% of the computer printer market (Bayt and Breuer, 2001). The biomedical industry is currently developing and using microfabricated fluidic devices for patient diagnosis, patient monitoring, and drug delivery. The i-STAT device (i-STAT, Inc.) is the first microfabricated fluidic device that has seen routine use in the medical community for blood analysis. Other examples of microfluidic devices for biomedical research include microscale flow cytometers for cancer cell detection, micromachined electrophoretic channels for DNA

fractionation, and polymerase chain reaction (PCR) chambers for DNA amplification (Northrup, et al., 1995). The details of the fluid motion through these small channels, coupled with nonlinear interactions between macromolecules, cells, and the surface-dominated physics of the channels create very complicated phenomena, which can be difficult to simulate numerically.

In 1998 Santiago et al. (1998) demonstrated the first μPIV system–a PIV system with a spatial resolution sufficiently small enough to be able to make measurements in microscopic systems. This first μPIV system was demonstrated measuring slow flows–velocities on the order of hundreds of microns per second–with a spatial resolution of $6.9\times6.9\times1.5\mu m^3$ (Raffel, et al. 2007). The measurement principle is based on Particle Image Velocimetry for large scale applications. The optical velocimetry technique uses conventional microscopy and digital imaging methods for the quantitative determination of two-component velocity data in a two-dimensional measurement plane. Depending on the choice of microscope objectives regions of investigation range from 1×1 mm^2 for a 5×magnification lens to 50×50 μm^2 for a 100×magnification lens. Within the region of interest velocity information spacing is of order 1μm. Spatial resolution up to a few 100 nm can be achieved (refer to review paper by Lindken et al., 2009).

For the optical measurement technique a transparent working medium and optical access to the area of investigation is needed. The flow is seeded with tracer particles for the visualization of the motion of the fluid. Ideally the tracer particles should follow the flow. This is achieved by matching the density of the fluid and of the flow-tracing particle or by the use of very small particles.

A volume of liquid with tracer particles is illuminated and observed with the aid of a microscope objective. For volume illumination all tracer particles emit light, but only the light originating from tracer particles in the focus plane of the microscope objective (and of those slightly out of focus) is collected by the objective lens and the position of those tracers is captured on a digital camera at one instant of time t_1. After a short time interval Δt the tracer particles are illuminated again and their position is recorded on a second digital image at time $t_2=t_1+\Delta t$. Please note that during the imaging process the three-dimensional particle positions are projected onto a two dimensional image plane where they form a two-dimensional particle image pattern. When there is a flow the positions of the tracer particles have slightly changed in the two consecutive recordings. The tracer particles with velocity v have shifted by a certain displacement Δs and hence, $v=\Delta s/\Delta t$. The two digital images are sent to a PC, where they are stored together with the time information. In a successive evaluation step the particle displacement Δs is digitally evaluated from the image pair.

For the purpose of data acquisition, a typical μPIV realization consists of a pulsed light source that is synchronized with the digital camera by a timing unit. The synchronization is done in a way that the first light pulse is set at the end to the first camera recording and the second pulse is set at an arbitrary time in the second recording. In this way the time interval Δt is independent of the camera frame rate, but defined by the time interval between the two synchronized light pulses. The time interval can now be adjusted to the flow conditions.

Frequency doubled Nd:YAG lasers at 532 nm wavelength of the laser light are a standard pulsed light source for PIV. For μPIV applications less than 10mJ of laser power per pulse is sufficient. Double cavity lasers consist of two lasers that can be triggered independently and of a beam-combining optic for the adjustment of the overlap of the two laser beams. Frequency-doubled Nd:YAG lasers are robust, have a good beam quality and the light can easily be coupled into the standard beam path of a microscope. Alternative light sources are diode-pumped lasers like Nd:YLF lasers that have a longer pulse length. This increases the signal intensity of fluorescent tracers. Ongoing development of laser diodes and high-power LEDs will increase the applicability of these types of light sources when used to illuminate μPIV recordings.

For a high image quality the camera should have the highest possible sensitivity/quantum efficiency. If the signal quality is insufficient intensified CCD cameras are an alternative but the image quality of intensifiers is poor. The use of double-shutter cameras reduces the time interval between two consecutive recordings to 1μs allowing measurements of high velocities at high magnification. The quality of a μPIV recording is significantly improved by fluorescence imaging.

Fluorescent tracer particles are added to the flow. Fluorescence is exited by illumination with monochrome laser light and the tracer emit light shifted to a longer wavelength, while all other obstacles like the walls of the microchannel reflect and scatter light at the original wavelength. An optical filter in the microscope is placed between the light collecting objective and the digital camera. The optical filter reflects light at the illumination wavelength and transmits the fluorescent light that has a longer wavelength. With this optical setup, light originating from the fluorescent tracer particles is collected on the camera sensor, while light originating from the channel walls and other non-fluorescent disturbances is blocked by the optical filter. This significantly improves the signal to noise ratio of the µPIV measurement.
A schematic of a µPIV set-up is shown in Figure 17 (for detail refer to Lindken et al., 2009).

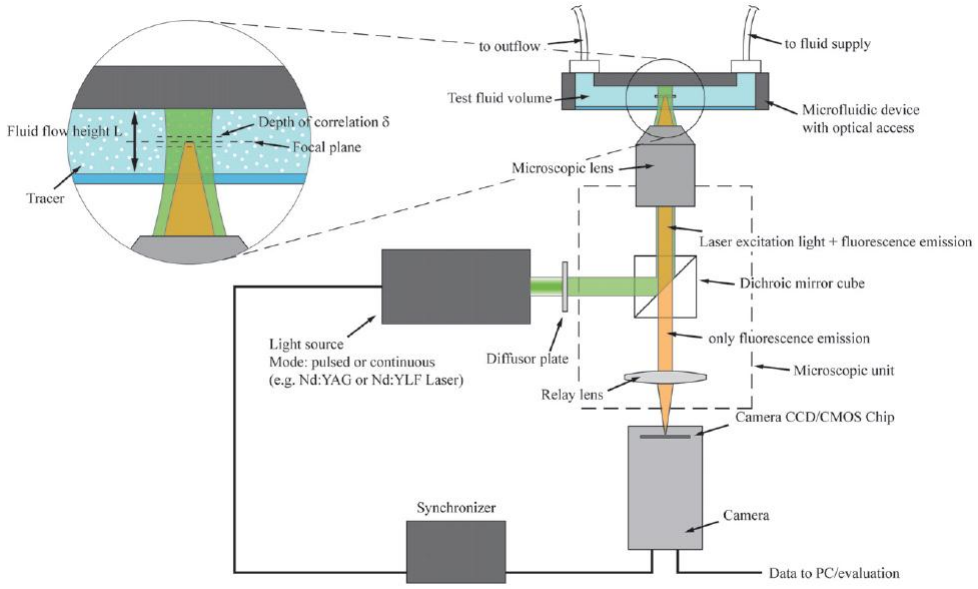

Figure 17: Schematic of a µPIV setup (Lindken et al., 2009).

Currently, applying the advanced techniques, the maximum spatial resolution of this technique stands at approximately 1μm. By using smaller seed particles that fluoresce at shorter wavelengths, this limit could be reduced by a factor of 2 to 4 (Raffel et al., 2007). Still higher spatial resolutions could be obtained by adding a particle tracking step after the correlation-based PIV. Spatial resolutions of an order of magnitude smaller could then reasonably be reached.
The various μPIV apparatus and algorithms have been demonstrated to allow measurements at length scales on the order of 1μm, significantly below the typical Kolmogorov length scale. These spatial resolutions are indispensable when analyzing flows in microdomains or the smallest scales of turbulence. The most significant problem standing in the way of extending μPIV to gas phase flows is seeding. With adequate seeding, it can be extended to gas flows. The significant issues associated with gas phase flows and microchannel flow are further explored by Meinhart et al. (2000, 1999).

Errors in PIV

PIV measurements contain errors arising from several sources which are mentioned below (Prasad, 2000):
(1) *Random* error due to noise in the recorded images.
(2) *Bias* error arising from the process of computing the signal peak location to sub-pixel accuracy.

(3) *Gradient* error resulting from rotation and deformation of the flow within an interrogation spot leading to loss of correlation.
(4) *Tracking* error resulting from the inability of a particle to follow the flow without slip.
(5) *Acceleration*error caused by approximating the local Eulerian velocity from the Lagrangian motion of tracer particles.
Certain errors can be minimized by careful selection of experimental conditions (for example, tracking error). However, other sources are inherent to the nature of the correlation in PIV and cannot be eliminated. For example, even if the recorded images are free from noise, the location of the correlation peak can be influenced by random correlations between particle images not belonging to the same pair. In addition, bias errors result from a phenomenon called pixel-locking in which the signal peak location is biased towards the nearest pixel while using a curve-fit or centroiding schemes to locate the discretized signal with sub-pixel accuracy. Similarly, gradient errors will occur in turbulent flow. Finally, acceleration error cannot be eliminated because of the very principle of PIV which uses the Lagrangian motion of particles to approximate the instantaneous Eulerian flow velocity.
Previous work has shown that random errors in PIV usually scale with the particle image diameter (Adrian, 1991).

$$\sigma_{\text{random}} = cd_e,$$

where d_e is the effective particle image diameter, and c is a constant whose value is between 0.05 and 0.10 depending upon experimental conditions(Prasad, et al., 1992; Boillot and Prasad, 1996).
Bias errors arise during the process of calculating the particle displacement to sub-pixel accuracy. Essentially, the correlation field is available on a discretized grid (typically 32×32). The location (S_x, S_y) of the maximum value in the correlation field will correspond to the particle displacement, but obviously, such a displacement will be an integer pixel value. In order to reduce measurement error, one attempts to locate the peak with sub-pixel accuracy using either a curve-fit method or a centroiding scheme. Unfortunately, any such scheme causes both random errors and bias errors. Experience shows that while centroiding schemes perform poorly on both counts in comparison to a parabolic or Gaussian curve-fitting, the latter can also cause significant bias errors.
The term bias error was coined to describe the phenomenon of pixel-locking, i.e. during the process of determining the displacement to sub-pixel accuracy, the resulting value is always biased towards the nearest integer-valued pixel (Prasad, et al., 1992). Bias error is zero if the particle is displaced exactly n pixels or n + 0.5 pixels, where n is an integer. For displacements $n<\Delta x<n$ +0.5 pixels, the measured displacement is biased towards n, and for n+0.5<Δx<n+1 pixels, the measured displacement is biased towards n+1. The situation is depicted in Figure 18 where a linear velocity profile (Couette flow) actually gets measured as a 'staircase' profile. The true and measured values coincide at integer and at half-pixel values.

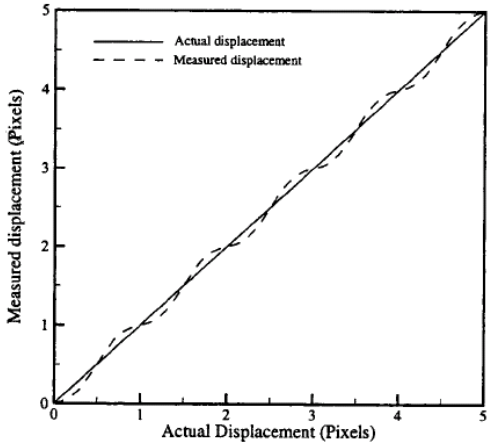

Figure 18: Bias error due to pixel-locking.

It is of course possible to predict the amount of bias error using modelling or measurement, implying that it should be possible to develop a look-up table to retrieve the correct displacement from the measured displacement just by subtracting the appropriate value of the bias error. Unfortunately, any measured result will also include random, gradient, and acceleration errors in addition to bias error. By their very nature, these other errors are not deterministic. Bias error may therefore only be corrected if it greatly dominates over the other errors. Bias errors, if present, become very apparent when histograms of displacements are plotted. Pixel-locking is seen when data-points gather in clusters near integer pixel values. Bias errors become large when the particle image diameter approaches *small* values (≈1 pixel). On the other hand, random errors increase when d_e increases. A suitable compromise, as verified by several practitioners, is to keep d_e at about 2 pixels.
In typical flows, particle streamlines are not straight, but curved. Consequently, an error is incurred when the Eulerian velocity is approximated using Lagrangian particle displacements as depicted in Figure 19.

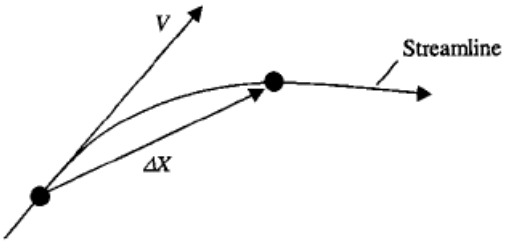

Figure 19: Acceleration error: approximation of the local Eulerian velocity using Lagrangian particle displacement.

It is easy to see that if the pulse separation Δt is larger, then so is Δx, and greater is the deviation of the measured velocity from the true velocity. This suggests that one must reduce Δt. On the other hand, if one were to reduce Δt too much, the measurement of Δx becomes difficult; at very small values of Δt, it may become impossible to distinguish Δx from random error. Obviously, simple error considerations suggest that the fractional random error can be reduced only by increasing Δx, and correspondingly Δt. So what is the value of Δt at which the overall error is minimized? The optimal pulse separation was derived (Boillot and Prasad, 1996) as:

$$\Delta t_{\text{opt}} = \sqrt{\frac{2\sigma_{\text{random}}}{Ma}} = \sqrt{\frac{2cd_e}{Ma}},$$

where a is the local acceleration of the particle. Of course, a is unknown until the flow is measured, therefore, a twostep measurement may be required, wherein the first measurement is conducted with a guessed Δt in order to determine a, followed by a second measurement with an optimized Δt. It should be mentioned that not all regions of a flow field possess the same value of a, hence, additional optimization may be necessary.

Applications

PIV technique has many application in different areas of research. Here, few of these applications are presented to show how this technique has spread out to many diversified research fields.

Boundary layer flows

1st case. Stereoscopic particle image velocimetry (SPIV) is applied to measure the instantaneous three component velocity field of pipe flow over the full circular cross-section of the pipe (see Figure 20, van Doorne and Westerweel, 2007). The light sheet is oriented perpendicular to the

main flow direction, and therefore the flow structures are advected through the measurement plane by the mean flow(see Figure 21). Applying Taylor's hypothesis, the 3D flow field is reconstructed from the sequence of recorded vector fields. The large out-of-plane motion in this configuration puts a strong constraint on the recorded particle displacements, which limits the measurement accuracy. The light sheet thickness becomes an important parameter that determines the balance between the spatial resolution and signal to noise ratio. It is further demonstrated that so-called registration errors, which result from a small misalignment between the laser light sheet and the calibration target, easily become the predominant error in SPIV measurements. Measurements in laminar and turbulent pipe flow are compared to well established direct numerical simulations, and the accuracy of the instantaneous velocity vectors is found to be better than 1% of the mean axial velocity. This is sufficient to resolve the secondary flow patterns in transitional pipe flow, which are an order of magnitude smaller than the mean flow.

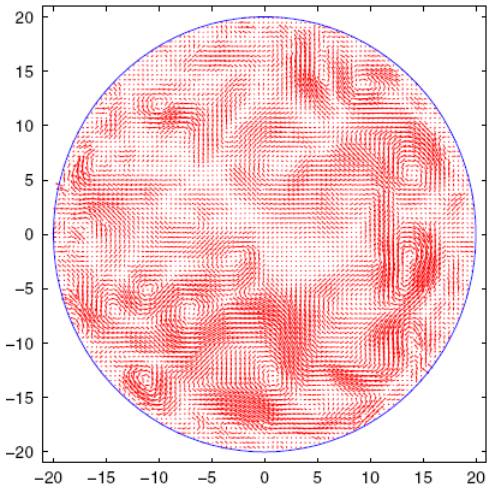

Figure 20: Example of the instantaneous turbulent flow field in a cross-section of the pipe. Displayed resolution is 8× 8 px, or 0.5×0.5 mm².

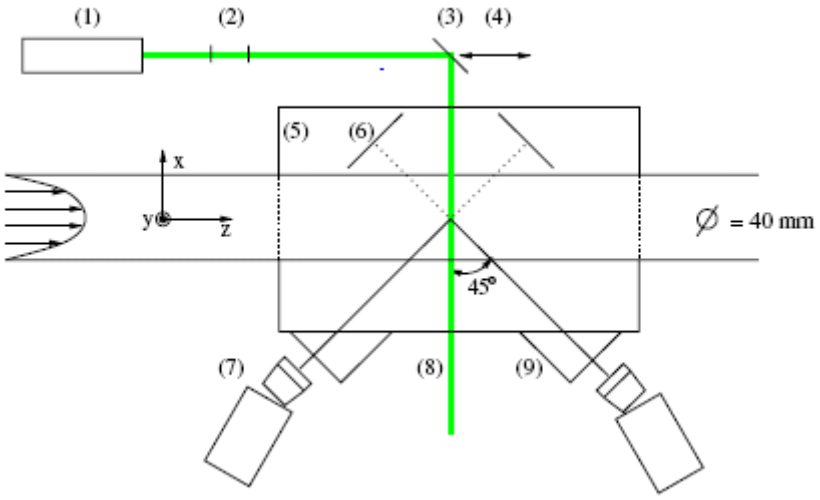

Figure 21: Schematic (top view) of the stereoscopic-PIV system. 1 Nd: YAG-laser, 2 lenses, 3 mirror on a micro-traverse, 4 traversing direction of the mirror, 5 test section, 6 anti-reflection screen, 7 CCD camera on Scheimpflug mount, 8 light sheet, 9 water prism.

2nd case. Stereo PIV measurements in streamwise-spanwise planes of a turbulent boundary layer was used (Longmire et al., 2001) to measure three instantaneous components of velocity.

The flow was seeded with olive oil droplets (nominal diameter 1μm) that were generated by 8 Laskin nozzle units set up in parallel. The oil droplets were ingested into the intake of the wind tunnel upstream of honeycomb straighteners and screens used for flow conditioning. At the test section, glass side-walls and a glass bottom wall were installed in the wind tunnel to provide high-quality optical access. The seed particles were illuminated by pulsed sheets from two Nd:YAG lasers (Big Sky CFR200) directed through one side window and oriented parallel with the bottom wall of the tunnel (see Figure 22). The laser pulse energy was 150mJ, and the thickness of each sheet was 0.15 mm. Sets of digital images were captured by two Kodak Megaplus dual-frame CCD cameras (1024×1024 pixels). A TSI synchronizer box was used to control the strobing and timing of the cameras and lasers. The cameras were aligned in a plane parallel with the spanwise-wall-normal flow plane and inclined at angles of 15° to the wall-normal direction as shown in Figure 22. Since the object plane was not parallel to either lens plane, the perspective view caused a geometric distortion. To overcome this problem, the Scheimpflug condition that requires the object, the lens, and the image plane to intersect at a common line was enforced. This arrangement introduces strong perspective distortion and varied magnification across the image, requiring that the camera configuration be calibrated for each measurement location.

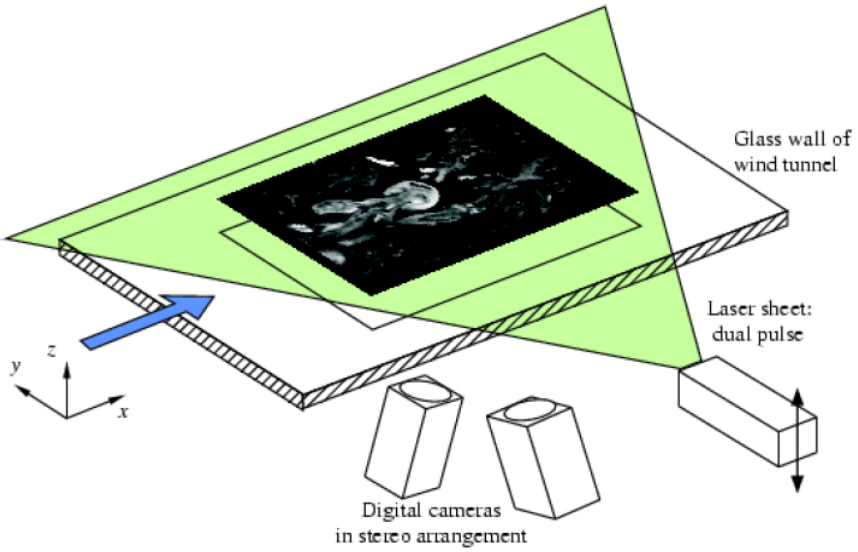

Figure 22: Experimental set-up.

The measurements had two major sources of uncertainty. First, the Gaussian peak fit in the cross-correlation algorithm generated an uncertainty of approximately 0.1 pixels. Second, a residual error arises due to the least square curve fit in solving the four pixel-displacement equations in three unknowns. This residual error can play a major role in the uncertainty if concentration gradients in seeding occur within the flow field. In this experiment, such gradients were not significant, and this error was on average about half of the Gaussian error. A maximum value of 0.2 pixels was observed.

Velocity gradients were computed on each reconstructed vector grid using a second order central difference scheme wherever possible in the domain and a first order forward or backward difference at the boundaries. To identify the swirling motion or the eddies in the flow field, a quantity called the swirl strength λ_{ci} (Zhou et al., 1999) which is the magnitude of the imaginary part of the eigenvalue of the local velocity gradient tensor was used. Since the PIV images are planar, only the in-plane gradients and form a two dimensional form of the tensor was used. Vortices can be identified by extracting iso-regions of λ_{ci} (Adrian, Christensen & Liu, 2000). Sample plots from an instantaneous flow field where the local mean velocity (U_c=0.65U_∞) has been subtracted are given in Figure 23.

The images acquired covered an area of 1.2δx1.2δ (δ being the boundary layer thickness) with the overlap area (region in which the three components of the velocity field are computed) being 1.0δx1.0δ. Each data set consisted of 750 images captured at a rate of 15Hz. The seeding particles had a nominal size of 2-3 pixels in diameter. The images were blurred to reduce the effect of noise and to eliminate pixel bias. To enhance the quality of the computed vector fields, interrogation spot windows in each image pair were offset by the mean pixel displacement of ~4 pixels while performing all cross correlations.

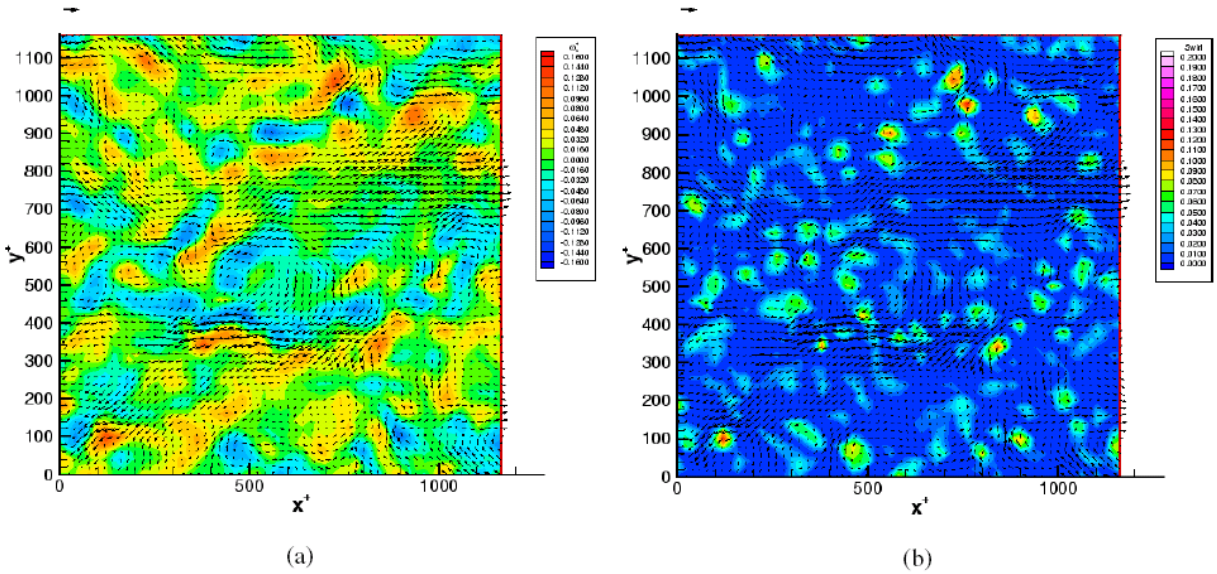

Figure 23: Streamwise-spanwise plane at $z/\delta = 0.09$ ($z^+ = 92$): (a) vorticity, (b) swirl strength.

Supersonic flows

1st case. Tomographic particle image velocimetry and proper orthogonal decomposition are used by Humble et al., (2007) to investigate the three-dimensional instantaneous flow organization of an incident shock wave/turbulent boundary layer interaction at Mach 2.1.

Experiments were performed in the blow-down transonic-supersonic wind tunnel (TST-27) of the High-Speed Aerodynamics Laboratories at Delft University of Technology. The facility generates flows in the Mach number range 0.5–4.2 in a test section with maximum dimensions of 270mm×280mm. The Mach number is set by means of a continuous variation of the throat section and flexible nozzle walls. The tunnel operates at unit Reynolds numbers ranging from 30×10^6 to $130\times10^6 m^{-1}$, enabling an operating use of approximately 300s. In the this study, the tunnel was operated at a nominal Mach number of 2.1 (U_∞=503m/s) with a stagnation pressure of 282kPa and stagnation temperature of 273K. A schematic representation of the experimental arrangement is shown in Figure 24.

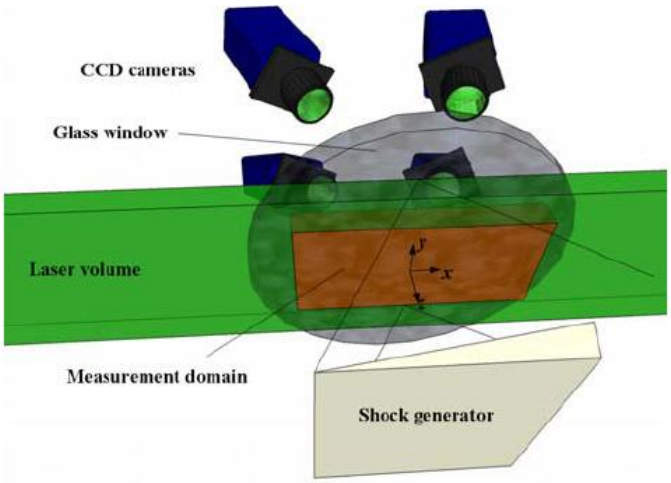

Figure 24: Schematic of experimental arrangement.

Flow seeding and illumination constitute critical aspects of PIV in high-speed flows. A 10mm diameter probe was inserted into the settling chamber to seed the upstream boundary layer. Titanium dioxide (TiO_2) particles with a nominal diameter of 170nm and a bulk density of 200kg/m^3 were adopted as tracers. The particle relaxation time across the incident shock wave (based on particles with a nominal diameter of 50nm) has been determined to be τ_p~2μs, corresponding to a frequency response f_p~500kHz (Humble, Scarano, & van Oudheusden, 2007). The seeded flow was illuminated by a Spectra-Physics Quanta Ray double-pulsed Nd:Yag laser, with 400mJ pulsed energy and a 6ns pulse duration at wavelength 532nm. A probe inserted into the flow downstream of the test section provided laser light access, and shaped the light beam into a volume using light optics. Before light entered the probe, a knife-edge slit filter was used to remove the low-energy fringes present, and to give a better approximation of a top-hat light intensity distribution. To minimize reflections, illumination was almost tangent to the wall. The laser pulse separation was 2μs, allowing a particle displacement in the freestream of approximately 1mm (≈20 voxels).
The tomographic results for revealing the 3D instantaneous structure of the interaction are depicted in Figure 25 which shows a series of uncorrelated measurement volumes containing instantaneous streamwise velocity. In this figure, Isosurfaces of streamwise velocity are shown; relatively high-speed ($0.9U_\infty$) in red, intermediate ($0.75U_\infty$) in green, and relatively low-speed ($0.55U_\infty$) in blue. Velocity vectors are shown flooded with streamwise velocity.

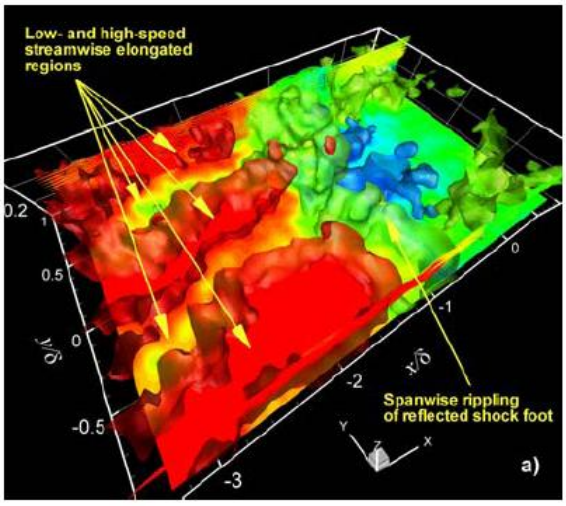

Figure 25: Instantaneous flow organization of the interaction.

2nd case. Before the Space Shuttle could return to flight after the loss of Columbia, NASA was required to validate the computational fluid dynamics (CFD) codes that it uses to predict the trajectories of debris that may be shed from the vehicle during launch. To meet this and other requirements, NASA conducted two tests of a 3% scale model of the Shuttle ascent configuration in the NASA Ames 9×7ft^2 Supersonic Wind Tunnel (9×7 SWT). In these tests, Dual Plane Particle Image Velocimetry (PIV) was used to measure the three components of velocity upstream of the Orbiter wings where debris shed from the External Tank (ET) would be convected downstream. The measurements were made in four cross-stream vertical planes located at different axial positions upstream of the Orbiter and above the ET. The measurements were made at two Mach numbers (1.55 and 2.5) over a range of model attitudes. The high stream velocity necessitated the use of the dual plane technique. These measurements revealed a complex network of interacting shock waves and a region of turbulent, separated flow on the ET just upstream of the Orbiter-to-ET attach point ("bipod"), where foam broke loose during Columbia's final flight.
Figure 26 shows average axial velocities in the most upstream measurement plane for a typical case. Higher spatial-resolution measurements were made in a single vertical plane in the separated-flow region above the Intertank section of the ET. More than 7000 samples were acquired at a single test condition to allow computing turbulence statistics. Figure 26 clearly shows the bow shock-wave from the nose of the External Tank (ET). The data are not laterally symmetric because the measurement plane was not perpendicular to the flow (it was yawed 15°). In addition, the cable tray on the starboard side of the ET ogive (Figure 26) probably induced flow asymmetry (more detail in Raffel et al., 2007).

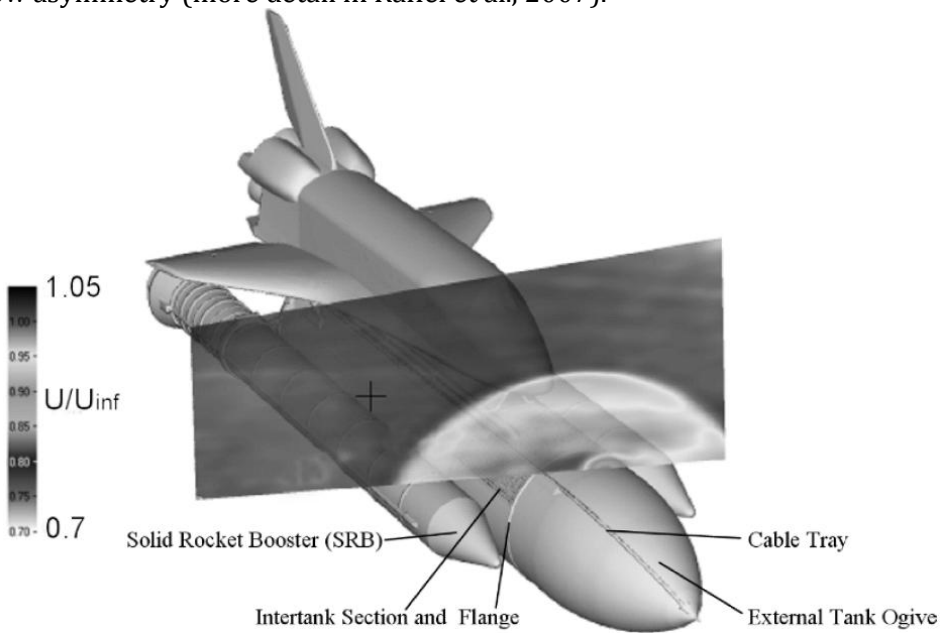

Figure 26: Sample plot of normalized axial velocity in the most upstream measurement plane $Ma_\infty = 2.5$, $\alpha = 0^\circ$, $\beta = 0^\circ$.

Transonic flows

1st case. Stereoscopic recording techniques were used by Woisetschläger et al. (see Raffel et al., 2007) to perform detailed studies of the unsteady rotor-stator interaction in a transonic turbine. A total number of 24 stator blades and 36 rotor blades were used in this turbine with rotational speeds between 9600 and 10600 rpm. The inlet flow temperature was between 360 and 403K. The turbine's control system (Bently Nevada) provided 12 TTL and one analog pulse per revolution. By combining both, a high resolution trigger signal was obtained. The details
of the camera arrangement are shown in Figure 27, with one camera axis being perpendicular to the light sheet and the second camera axis being inclined by 27° to the first. This angle was

limited by the geometry of the turbine casing. The cameras were mounted according to the Scheimpflug condition (see Figure 27).

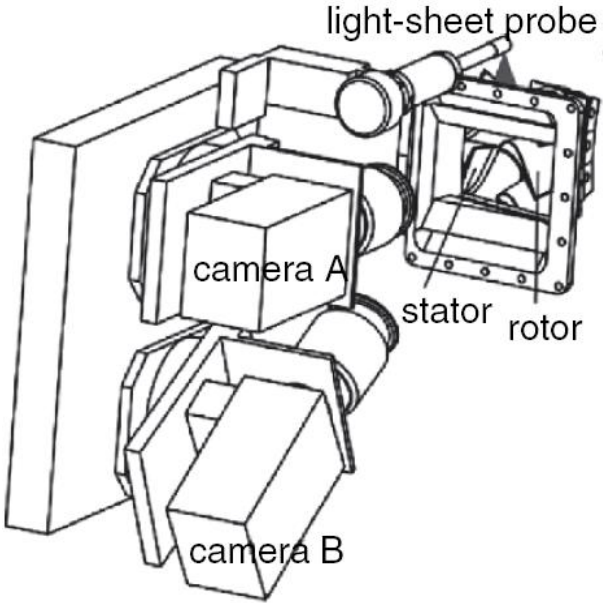

Figure 27: Optical set-up.

The light sheet probe was fixed to the cameras' base plate while a flexible silicon tube was used to seal the air inside the turbine. This rigid system eased focusing and calibration. The laser light was guided through an articulated arm to the light sheet probe. A high-temperature resin was used to glue the single elements, especially the cover glass (three component resin, R&G GmbH). This glass shielded the aligned optical prism against the fluctuating pressure caused by the flow. The light sheet was observed through a plan-concave quartz glass window (HERASIL; anti-reflection coated) with dimensions 123× 75 ×15mm^3 and a R = 264mm curvature on one side.
Seeding was provided approximately 500mm upstream the stator blades through a specially formed pipe (S-shape, 7mm inner diameter). In the most upstream part of the pipe a large number of holes with 1.8mm diameter were drilled ("shower head"). This part with a length of 130mm was aligned in a tangential direction upstream the light sheet.
Two results for the mean velocity (all three components) and the vorticity (from the two in-plane components) are presented in Figure 28. When looking at the vorticity one can observe seven phases of vortex shedding during one period of blade passing. This means the vortex shedding frequency is about 40 kHz. A detailed comparison with interferometric measurements indicated that the tracer particles used started to act as lowpass filter at about 80 kHz. Therefore, only the first harmonic of the vortex movement can be found in the PIV results. While high resolution CFD methods predict various shapes of vortices, PIV results showed vortices of more or less circular type because of the band-pass filtering. On the other hand, PIV provided the unique possibility to investigate the interaction between shocks, shock reflections, vortex shedding and wake-wake interaction in these turbulent and transonic flows. Further discussion of the results can be found in (Göttlich et al., 2004 & 2005; Lang et al., 2002; Woisetschläger, 2003 & 2003a). (Raffel)

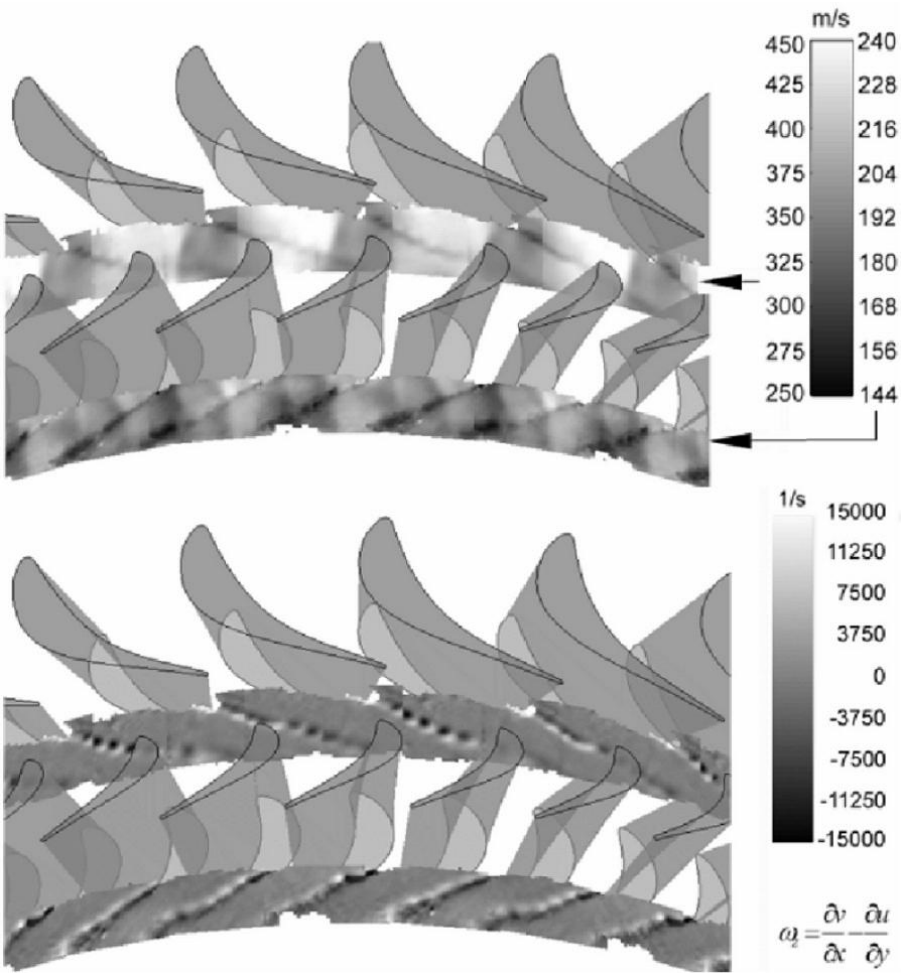

Figure 28: Velocity (upper image) and vorticity (lower image) at mid-span in a transonic turbine stage (10600 rpm).

2nd case. The application of PIV in high-speed flows (e.g.: transonic flow above airfoil) yields two additional problems: the resulting behavior of the tracer particles and the presence of strong velocity gradients. For the proper understanding of the velocity maps it is important to know how far (Raffel et al., 2007) behind a shock will the tracer particles again move with the velocity of the surrounding fluid. Experience shows that a good compromise between particle behavior and light scattering can be found if this distance is allowed to be of the order of one or two interrogation areas. Strong velocity gradients in the flow will lead to a variation of the displacement of the images of the tracer particles within the interrogation area. This influence can be reduced by application of image shifting, that is by decreasing the temporal separation between the two illumination pulses and increasing the displacement between the images of the tracer particles by image shifting to the optimum for evaluation. This is especially important if autocorrelation and optical evaluation methods are applied as in this case it is required to be able to adjust the displacement of the tracer particles to the range for optimal evaluation (i.e. $\approx$200 μm).

Strong velocity gradients are present in flow fields containing shocks. Figure 29 shows such an instantaneous flow field above a NACA 0012 airfoil with a chord length of C_l =20cm at Ma_∞= 0.75 (Raffel and Kompenhans, 1993). By subtracting the speed of sound from all velocity vectors the supersonic flow regime and the shock are clearly detectable.

Figure 29: Instantaneous flow field over a NACA 0012 airfoil at α = 5 degree.

PIV in Shock tubes and shock tunnels

Shock tubes and shock tunnels generate compressible flows that are characterized by short time durations and large gradients. Therefore, these flows are a challenging application for all kinds of measurement systems. Additionally, a high information density is desirable for each experiment due to short measurement times. During recent years, particle image velocimetry (PIV) was therefore extensively tested and successfully applied to different flow configurations in the shock-tube department at "French-German Research Institute of Saint-Louis (ISL)". It turned out that one difficulty common to all shock-tube or tunnel applications is a good timing and triggering of the PIV system. An appropriate seeding is another crucial factor. The latter is particularly difficult to manage because, in contrast to continuous facilities, no assessment of the seeding quality is possible before and during the experiment.

The experimental setup with the shock tube and the PIV system as reported by Havermann et al. (2008) is depicted in Figure 30. Particle seeding was accomplished by a smoke generator burning incense resin that gives a typical smoke particle diameter of approximately 1 µm. Both the open-end tube and the ambient air near the opening were seeded before each experiment. The PIV system was triggered by a pressure transducer located close to the shock-tube opening.

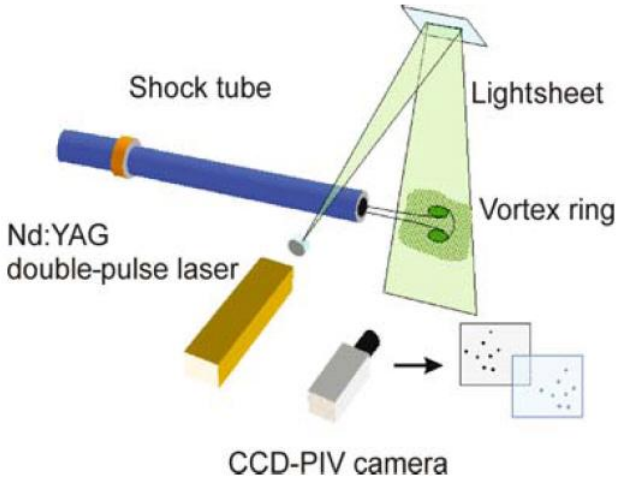

Figure 30: PIV setup

The PIV data analysis was performed for a 36×36 pixel interrogation window size using the inhouse software. Despite a low particle concentration in the core region a velocity measurement was obtained. First, the horizontal velocity component in the laboratory coordinate system is plotted (Figure 31). Masked regions are automatically blanked by selecting a certain noise level of the correlation function. The vectors indicate the strong rotation of the flow around the vortex cores. If the propagation velocity of the vortex ring is subtracted from the original data, the velocities in a vortex-fixed coordinate system are given, which allows the plot of streamlines to be made (not shown here).

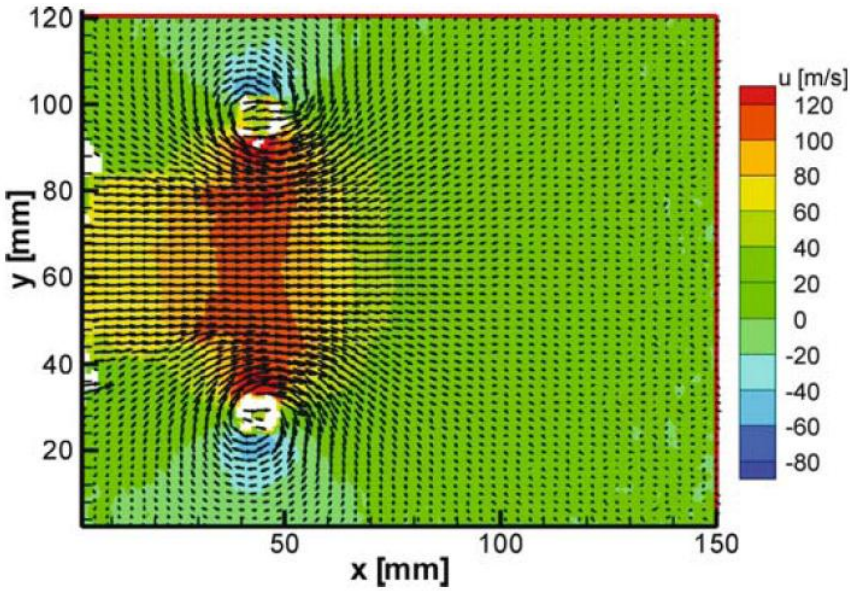

Figure 31: Horizontal velocity component and vector field for the laboratory-fixed frame.

PIV has been applied to a large variety of simple and complex flows in short duration facilities (shock tunnel and shock tube) at ISL. For rather simple flow fields with a low level of turbulence the instantaneous PIV results represent the flow field very well even with rather large interrogation window sizes. Velocities up to nearly 2km/s have been measured in a shock tunnel with an accuracy of a few per cent comparing the experimental results with analytical and theoretical values. This confirms the ability of PIV to be used for CFD validation even in a very high velocity range.

PIV in naval hydrodynamics

Particle image velocimetry is introduced as an essential tool for flow diagnostics in the field of naval hydrodynamics. In the particular field of naval hydrodynamics, PIV has seen its range of applications widely expanded in recent years: underwater vehicle flows, ship wake (Gui et al., 2001), ship roll motion (Di Felice), propeller flow (Cotroni et al., 2000), wave breaking, freak waves, free surface flows (Dabiri, 2003), bubbly flows, boundary layer characterization for drag reduction by microbubbles, sloshing flows, waterjets, etc.

A review of the existing systems and their use in typical industrial-type problems in the naval field is briefly presented (for detail refer Di Felice and Pereira, 2008) with four cases of particular relevance: 1. Unsteady flow around the bilge keel of a ship in damped roll motion, for CFD model development; 2. propeller flow survey in a cavitation tunnel, using phaselocked measurements, for the identification of noise sources; 3. wake survey of a large underwater vehicle model, for the purpose of design validation; 4. bubble transport in a propeller flow, for the purpose of noise reduction and propeller performance.

The PIV technique will typically be used in the framework of ship and propeller model testing, both in cavitation and towing-tank facilities. In most towing-tank institutions, the ship model

length ranges from 3 to 8m and the diameter of the propeller model is within the range 130 to 350 mm. These features provide the basic requirements for the size of the measurement area and for the spatial resolution of the PIV system. On one hand, the measurement area should cover the complete crossflow area of the propeller, with an additional 10 to 20% margin to map the full slipstream. On the other hand, and together with the previous requirement, the system should be able to resolve the thin blade wake that is usually of the order of a few millimeters. For a long time, the resolution of the PIV sensors and/or the power of the laser sources would not allow these two conditions to be satisfied simultaneously. The only practical approach was to make a compromise between spatial resolution and measurement area or, alternatively, to patch multiple high-resolution areas into a larger one, at the cost of additional running time. These end-user needs have motivated the hardware manufacturers to improve the performance of the PIV components, especially in the area of the imaging sensors: the sensitivity is being continually enhanced and very high resolution (4 Mpixels and more) PIV cameras are now commercially available. On his side, the end-user has put the effort on the development of advanced PIV algorithms that would contrast the hardware limitations. The combination of techniques such as window offset, iterative grid refinement, window deformation and other algorithms now enables the reconstruction of velocity gradients from interrogation windows as small as 16×16 pixel, without compromising the accuracy.

In cavitation facilities, the presence of two-phase flows introduces new practical and technological challenges. The measurements in these instances have been so far performed in off-cavitation conditions to avoid camera blooming and consequent sensor damage. Cavitation manifests itself by the occurrence of gas/vapor structures of various types: submillimeter (10 to 100 μm) cavitation bubbles convected by the flow, large vapor cavities attached to the solid boundaries (e.g., sheet cavitation on a propeller), vapor filaments (e.g., cavitating vortex at the tip of a blade or cavitating turbulent structures in the blade shear wake). To map the two phases simultaneously, fluorescent particles have long been suggested and used in laboratory-scale setups. However, their use in large facilities has not yet been assessed because of their small size and low scattering efficiency, both factors hindering their detection from distant imaging systems, as well as their prohibitive cost and progressive efficiency decay over time. Safety issues related to their chemical characteristics, such as toxicity and chemical reactivity with other compounds present in the facility, are another major obstacle to their use in industrial- or commercial-type facilities.

Surface-Ship Flow

Particle image velocimetry is particularly well suited, as opposed to singlepoint measurement techniques like LDV, for flows characterized by large spatial instabilities. In these situations, a whole-field measurement approach is the only way to efficiently address the problem. The application described hereafter illustrates such a situation with the case of the flow created by a ship hull in free roll decay.

The experiments were carried out in the INSEAN (Italian Ship Model Basin, Via di Vallerano, Rome, Italy) towing tank no. 2. The tank is 250m long, 9m wide and 4.5m deep, with a maximum carriage speed of 10m/s. A 5720-mm length frigate model (INSEAN model C2340) comprising of bilge keels is tested. A sketch of the experimental setup is shown in Figure 32. Two-component planar PIV measurements were performed using an underwater camera with a 1280×1024 pixel resolution. The lightsheet was fired at a rate of 12.5Hz, with an energy output of 200mJ per pulse, by a two-head Nd:YAG laser coupled with underwater optics. Roll being the only motion investigated in this experiment, the ship model was locked to the dynamic trim at an initial roll angle of 10° by means of a magnet-based release mechanism. A TTL trigger sequence was generated by a synchronizing device to pilot the Nd-YAG lasers and the camera acquisition system.

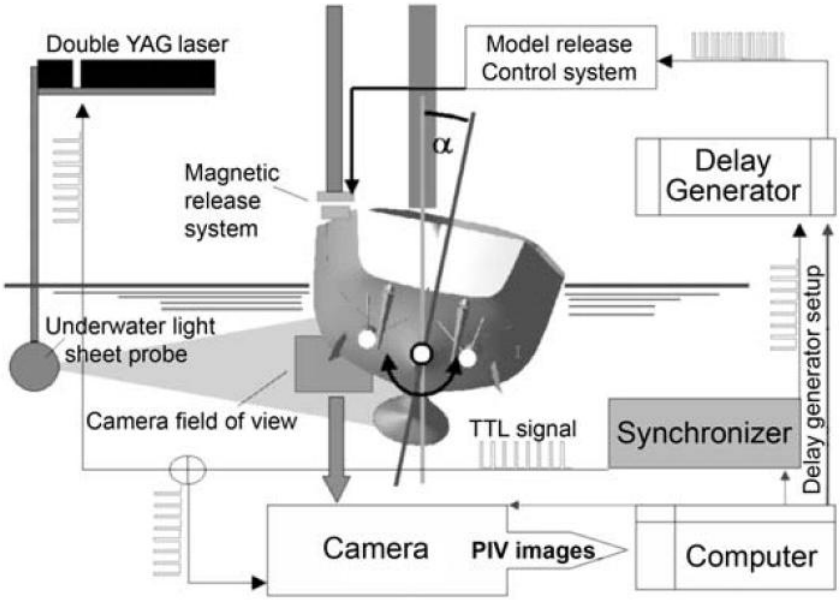

Figure 32: Surface ship flow: experimental setup.

The PIV analysis included the discrete offset technique and the iterative image-deformation method (Di Florio et al., 2002). The displacement field obtained with the first analysis method was used to distort the images (Huang et al., 1993), upon which direct cross-correlation was applied to calculate a corrected velocity field. This newly updated velocity predictor was subsequently used to redistort the original images and the process was repeated on an iterative basis until a convergence criterion could be verified. This type of iterative algorithm has been recently proved to be very efficient, accurate and stable (Scarano, 2002).

Propulsor Hydrodynamics

The first successful applications of particle image velocimetry to the propeller wake flow analysis appeared in the late 1990s (Cotroni et al., 2000 & 1999), in medium-scale facilities and for off-cavitation operation. The technique proved to be very well suited for this particular problem. Furthermore, the characteristic features of this flow, such as the strong velocity gradients and the presence of coherent vortex structures, have triggered the development of the iterative multigrid algorithms (Di Florio et al., 2002), which are now used on a standard basis in general PIV analysis.

The other measurements have been carried out in the INSEAN circulating water channel, a free-surface cavitation tunnel with a test section 10m long, 3.6m wide and 2.25m deep, capable of a 5.2m/s maximum flow speed. The shipmodel was a series 60 with a 6.096m length, propelled by a five-blade MAU propeller (diameter: 221.9mm). The experimental setup is shown in Figure 33. Underwater optics were used to produce the lightsheet from a Nd:YAG laser pulsing at 10 Hz with a 200mJ energy per pulse. The propeller angular position is given by a rotary 3600-pulse/revolution encoder to the synchronizer, which drives the two flashlamps and Q-switches of the two-head laser and the PIV cameras. The mean fluctuating velocity fields have been established on the basis of 129 PIV recordings phase-locked with the propeller angle, which was varied from 0 to 69° with a step of 3°. The stereo-PIV method uses two cameras that image the flow field from two different directions. Each camera measures an apparent displacement, perpendicular to its optical axis. Combining the information from both views, it is possible to reconstruct the actual three-dimensional displacement vector in the plane. The angular displacement method is chosen, as opposed to the translation method (Prasad & Adrian, 1993).

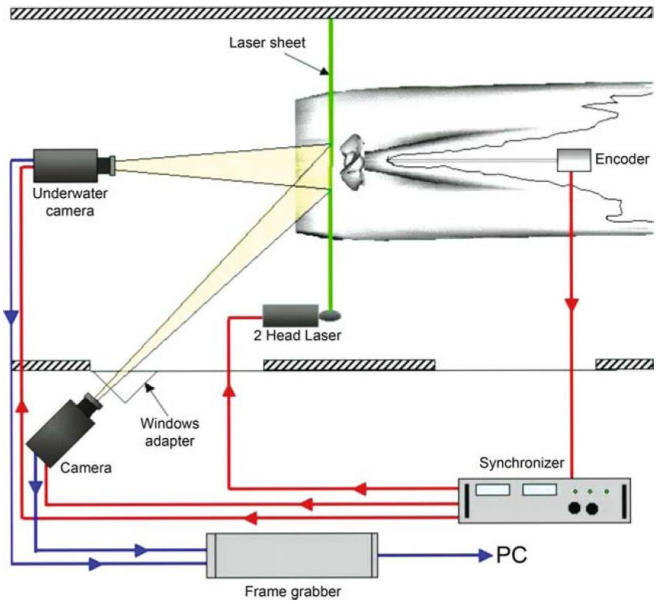

Figure 33: Propulsor hydrodynamics: experimental setup.

The propeller wake, observed at x/L = 0.9997, presents a number of features well outlined in Figure 34, which represent, the mean three-dimensional flow field (averaged over 129 instantaneous 3D vector fields), vectors represent the crossflow field (one every two vectors represented), contour represents the axial velocity magnitude. For a complete discussion, refer to (Calcagno et al., 2005). Note that Figure 34 is the first published stereoscopic PIV measurement in naval hydrodynamics.

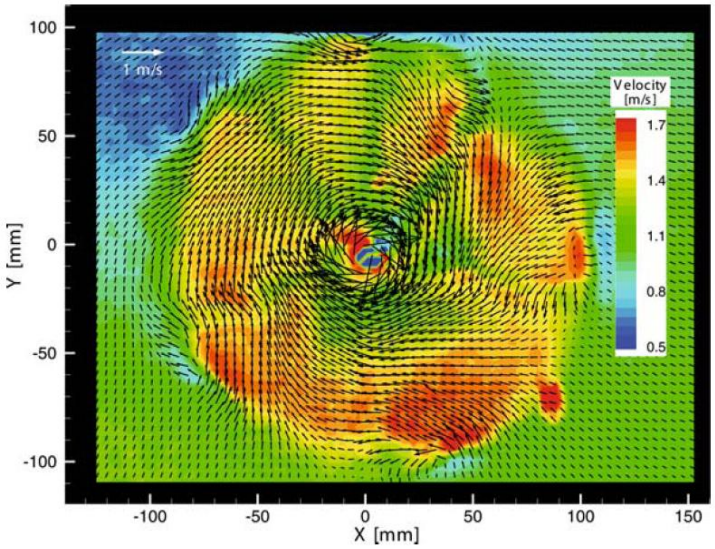

Figure 34: Near-propeller wake: mean three-dimensional flow field.

Underwater Ship Flows

A unique, highly modular and flexible underwater system for stereoscopic particle image velocimetry measurements has been devised at INSEAN for planar three-dimensional velocity measurements in large-scale facilities such as water tow tanks and tunnels (Pereira et al., 2003). The underwater stereo-PIV probe is designed in the form of modules that can be assembled into different configurations. Figure 35 shows the probe in its principal configuration, referred to as the design configuration. The probe, when fully assembled, forms a streamlined torpedo-like tube with an external diameter of 150 mm. The tube can be rotated about its axis in steps of 15°, and is rigidly linked to a bench through two hydrodynamically optimized struts. The whole

system can be attached to the tow-tank carriage or to a traversing system. The components are: 1. two struts; 2. two waterproof-camera sections; 3. two camera mirror sections, opened to water; 4. a waterproof section for the laser lightsheet optics; 5. a waterproof section for the lightsheet mirror; 6. the nose and tail sections, which have a semi-ellipsoidal shape.

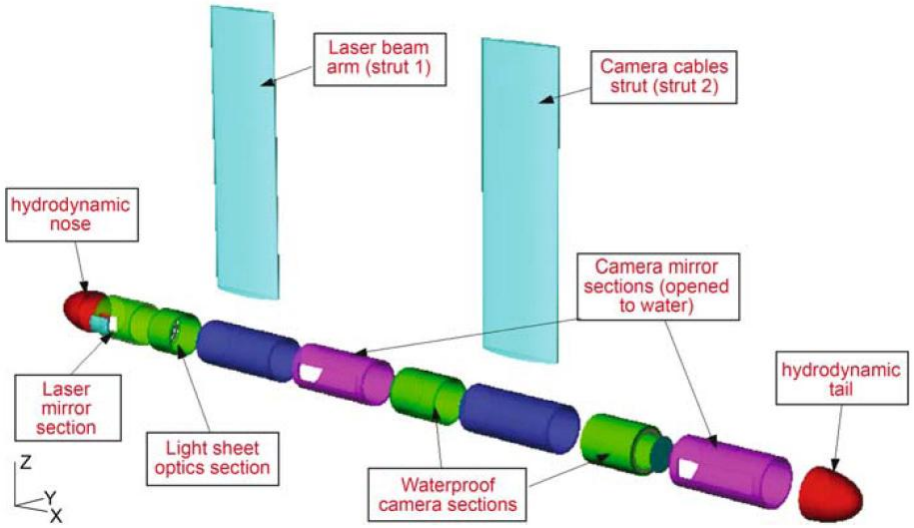

Figure 35: INSEAN's underwater stereoscopic PIV probe

The system is applied to the flow survey around a deeply submerged underwater vehicle model, referred to as UVM in the following sections. The experiments were carried out in the INSEAN towing tank no 1. The tank is 470m long, 13.5m wide and 6.5m deep, with a maximum carriage speed of 15m/s. The length of the model, made of glass-reinforced plastic, is 7.2m. The UVM is equipped with a 7-blade propeller with a diameter of 530 mm. The body was painted black and the propeller black-anodized to minimize the laser-beam reflections.
Figure 36 represents an overview of the UVM where the velocity magnitude in four planes (x/L=0.5, 0.625, 0.75, 1.05), normalized by the free-stream velocity is shown. The insets provide a detailed view of some important features of the flow: twin counterrotating vortex structures generated at the top of the sail, horseshoe vortex produced at the base of the sail, propeller phase-averaged field showing the accelerated flow. The test was carried out at a carriage velocity of 2m/s. Note that the measurements for the plane x/L=1.05 have been performed in phase with the propeller rotation in order to capture the flow features linked to the blades. A rotation pulse was generated for each revolution to trigger the stereo-PIV image acquisition, hence generating a dataset phase-locked with the propeller angular position.

Two-Phase Bubble Flows

Two-phase flows are another class of flows of great interest that require extended measurement capabilities. In fact, such a flow generally requires that both phases be measured in order to have a comprehensive insight into the physical mechanisms. Furthermore, flow three-dimensionality is a common feature in complex (real) flows, and a 3-component, 2D information as provided by a standard stereoscopic PIV approach can only provide a partial view of the global problem. The current efforts in the PIV community are related to the extension of the PIV concept to the full 3D space. A number of intermediate solutions have been developed, such as the multilayer PIV (Abe et al., 1998), scanning PIV (Brücker, 1997) or multiplane PIV (Kähler and Kompenhans, 2000). Holography (Meng et al., 2004) and defocusing digital particle image velocimetry (DDPIV) (Pereira and Gharib, 2002; Pereira et al., 2006) provide true volumetric information.

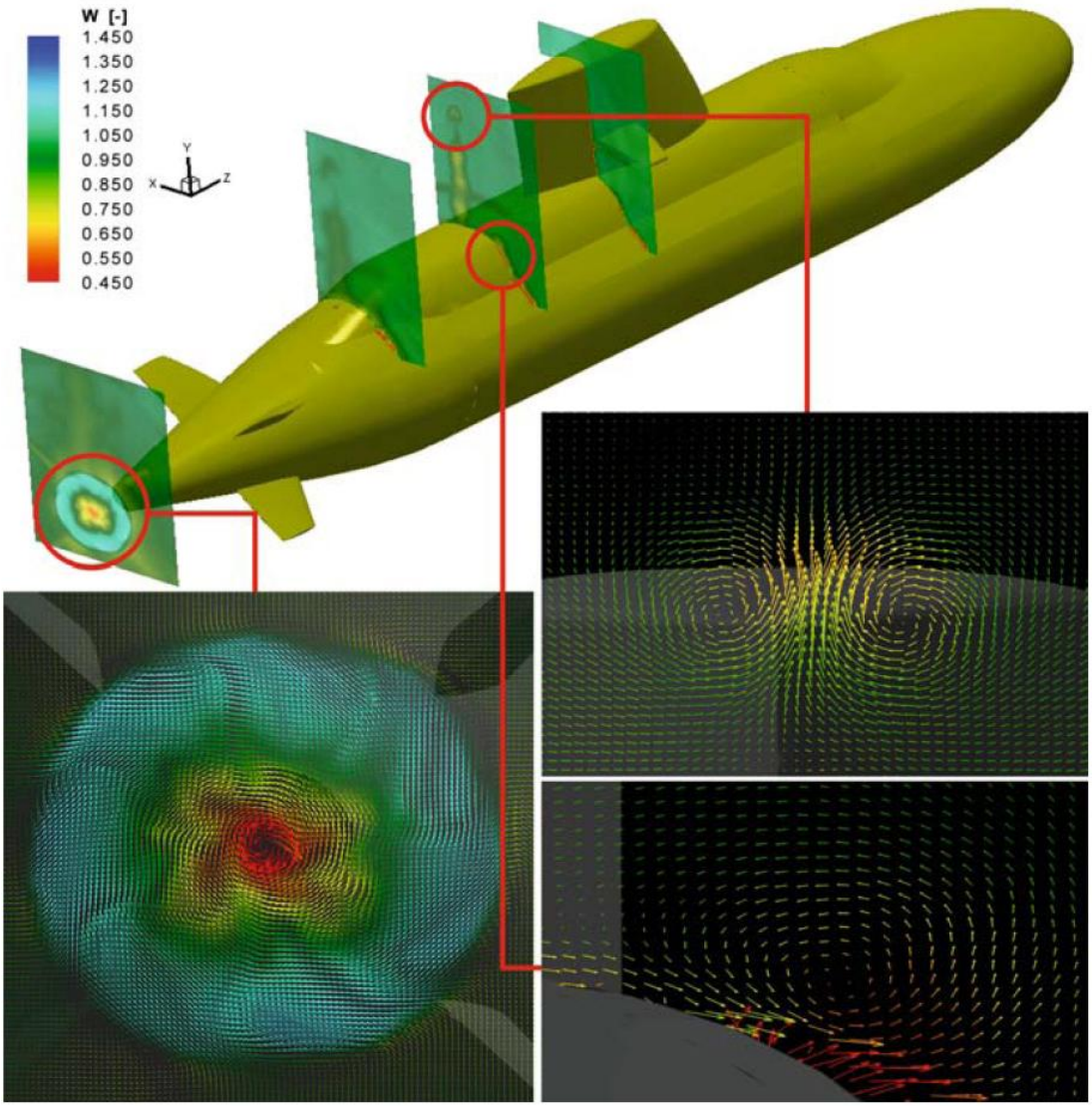

Figure 36: Overview and detail of the velocity field; four crossflow velocity fields are represented: x/L=0.5, 0.625, 0.75, 1.05.

The defocusing DPIV is here applied to investigate the collective bubble interaction with the flow induced by a propeller and, more specifically, their interaction with the vortex system generated by the blades. The experiments are performed in a laboratory water channel, as shown in Figure 37. The test section is 1000×150×150mm^3. The upstream flow velocity is 45cm/s. A bubble generator, placed upstream in the convergent section, generates a dense cloud of submillimeter air bubbles, which are used as flow markers. The two-blade model boat propeller has a diameter of 67mm. The rotation speed is set to 15 rps (3.16m/s at the blade tip). The measurements are locked on the propeller rotation for phase averaging. Flow mean quantities (velocity and vorticity) and second-order statistics (Reynolds' tensor) are calculated on sequences of 200 velocity vector fields. The DDPIV camera is a self-contained instrument that allows the capture of the three-dimensional information of the flow. It is composed of three apertures arranged according to a specific geometry. A 1600×1200 pixels CCD sensor, with an 8-bit resolution, is mounted behind each aperture to collect the light scattered by the flow markers (bubbles in this experiment). Sample results (not shown here), depicting the volumetric three-dimensional velocity vector field combined with the measurement of the bubble local density.

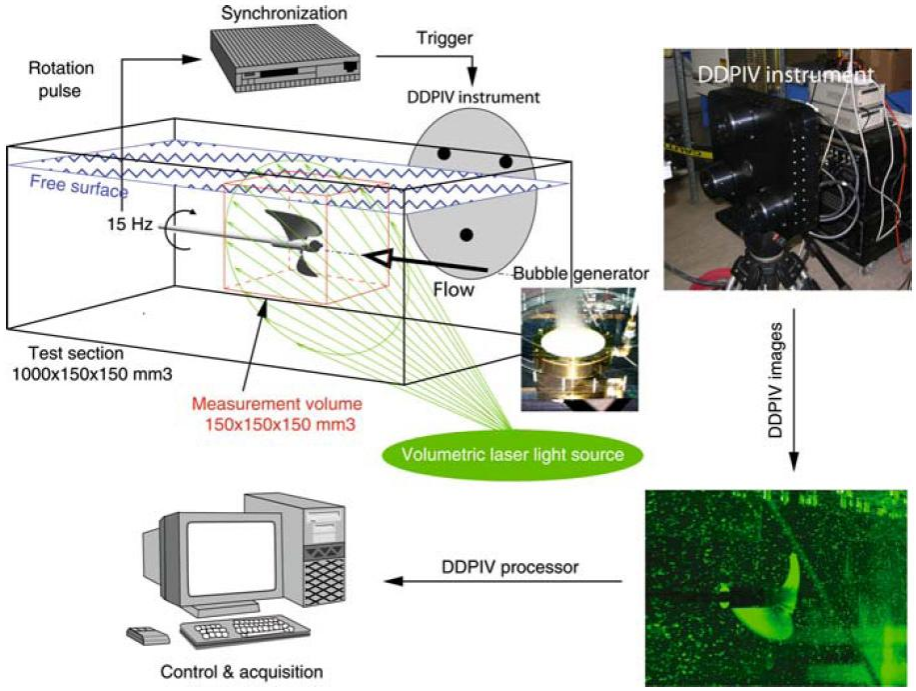

Figure 37: Bubbly flows: experimental setup.

The above mentioned techniques give the reader the opportunity to have a general overview on the state-of-the-art of PIV applications in the field of experimental naval hydrodynamics. For detail refer to Di Felice and Pereira (2008).

PIV in helicopter aerodynamics

1st case. With increasing use of civil helicopters the problem of noise radiation has become increasingly important within the last decades. Blade vortex interactions (BVI) have been identified as a major source of impulsive noise. As BVI-noise is governed by the induced velocities of tip vortices, it depends on vortex strength and miss-distance, which itself depends on vortex location, orientation, and convection speed relative to the path of the advancing blade. Blade vortex interaction can occur at different locations inside the rotor plane depending on flight velocity and orientation of the blade tip path plane.

To better understand and to model the development of rotor blade tip vortices, earlier velocity measurements were obtained using intrusive techniques such as hot-wires, but more recent flow measurements rely exclusively on optical techniques, mainly LDV (Boutier et al., 1996; Raffel et al., 1998) and PIV [Martin et al., 2000; van der Wall and Richard , 2005).

Recently, the wind tunnel measurements of rotor balde vortices has been performed on a rotor model of 4m diameter in the 6m×8m open test section of the Large Low-speed Facility (LLF) of the German Dutch Wind Tunnel (DNW) operated at 33 m/s (see Raffel et al. 2007). The helicopter rotor model used was a model of the MBB Bo 105 of the German Aerospace Center (DLR) Institute of Flight Systems in Braunschweig. The PIV parameters used for this investigation. The PIV system consisted of five digital cameras and three doublepulse Nd:YAG lasers with 2×320 mJ each, which were mounted, as sketched on Figure 38, onto a common traversing system in order to keep the distance between the cameras and the light sheet constant while scanning the rotor wake. The length of the traversing system was in the order of 10m, the height approximately 15m. Two stereo systems were used simultaneously. One system was equipped with 300mm lens in order to record a small observation area: 0.15m×0.13m, centered to the blade tip vortex and the second system was equipped with 100mm resulting of a field of view of 0.45m×0.38m. The large field of view was intended for an overview of the vortex and of the surrounding flow whereas the small field of view was intended for vortex analysis.

Conditionally averaged velocity and vorticity maps obtained by each stereo system are displayed in Figure 39. The results on the left were obtained with the large field of view stereo system. The blade tip vortex is clearly visible as well as the wake of the previous blade whereas on the small field of view on the right only the vortex can be seen but with a high spatial resolution.

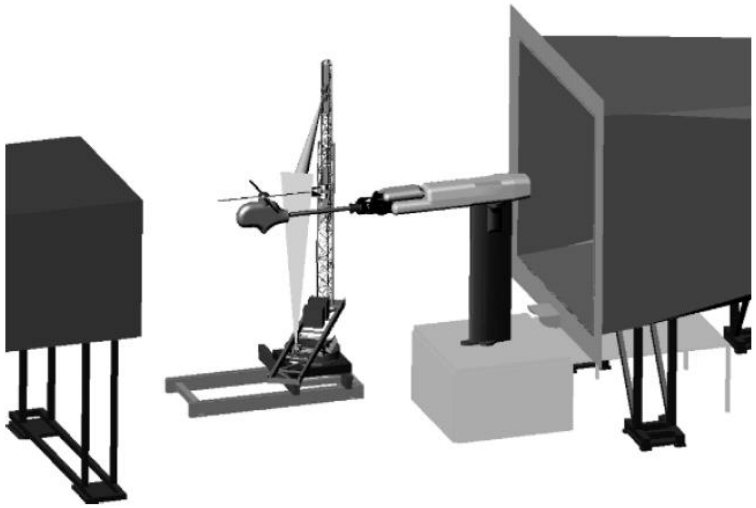

Figure 38: HART II stereoscopic PIV setup.

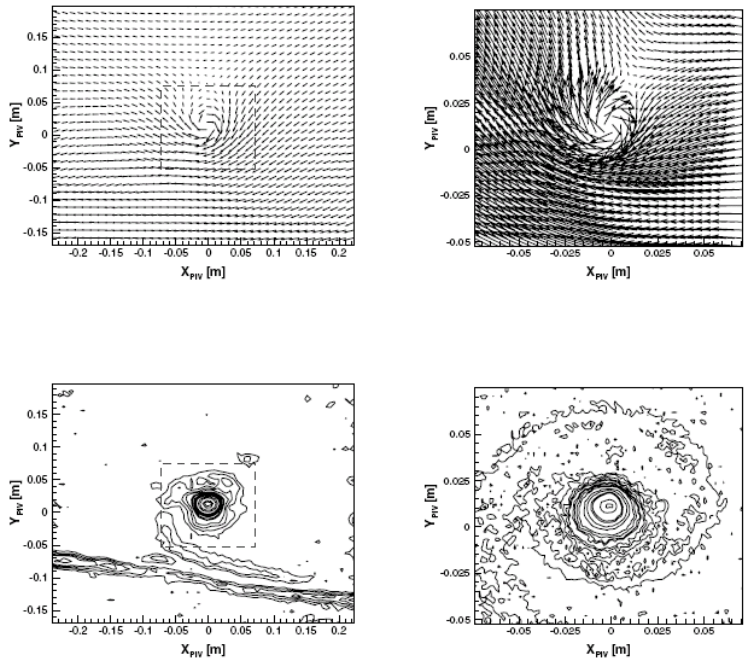

Figure 39: Averaged velocity (top) and vorticity (bottom) maps of a blade tip vortex; large field of view (left) and close-up view (right).

2nd case. Detailed studies of the boundary layer profile and the characteristics of the flow velocity distribution close to the leading edge of a helicopter blade profile were conducted using 2C-PIV (Raffel et al., 2007). The relatively small scales of flow structures related to dynamic stall, the study in which the flow field has been measured with a relatively high spatial resolution. The feasibility of μ-PIV measurements utilizing a mirror telescope in a wind tunnel has been demonstrated successfully. The spatial resolution of approximately 50μm allowed for an assessment of the different turbulence models and damping coefficients for the improvement of CFD predictions.

Stereoscopic PIV and pressure measurements have been performed to quantize the overall flow features close to the tip of a rotor blade, both in steady cases and during pitching motion. Two-components PIV measurements with an observation field size of 1mm and 50μm resolution, have been performed further inboard in order to resolve the relevant flow features in the phase shortly before the stall onset in steady and unsteady cases. The majority of the μ-PIV measurement has been made at a steady incidence angle of 11.5° . The development of the boundary layer, the reverse flow region and the shear layer towards the outer flow can clearly be seen in the result Figure 40.

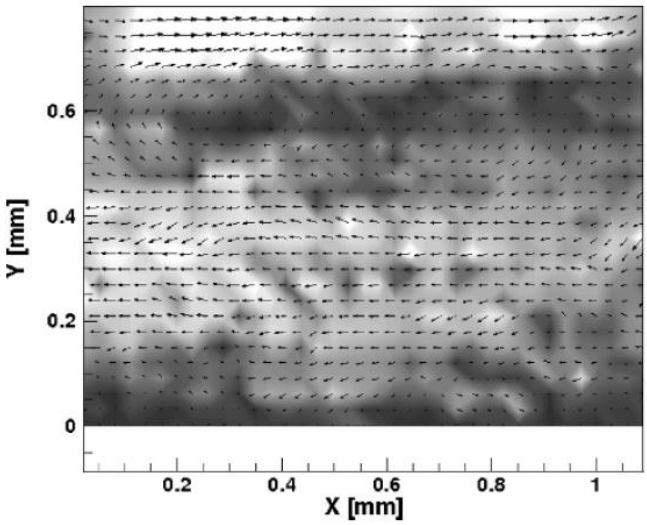

Figure 40: PIV results obtained with a mirror telescope objective at α=11.55°, steady case. The magnitude of the velocity has been plotted by gray levels. The coordinates x and y are given in millimeters. The origin is placed on the model surface (y), 5% chord length behind the leading edge (x).

Multiphase flow

Multiphase flows are present in numerous engineering applications. For better development of applied methods used in prediction and optimization of engineering flows a deep understanding of underlying flow phenomena is crucial. The studies reported by Chernoray and Jahanmiri (2011) and Chernoray et al. (2011) concerns dynamics of a two-phase flow around a rotating solid body. Under consideration is a model of a gear wheel in a gearbox which rotates and is partially submerged in oil (see Figure 41). The flow measurements are carried out by using particle image velocimetry and the test rig is specially designed for this purpose with the optical access maximized (see Figure 42). The flow similarity with respect to a real gearbox is fully maintained and the working fluid is a transparent mineral oil. The PIV measurements are performed at four different rotation speeds for two different wheel configurations in order to cover a spectrum of operational conditions needed for numerical modelling. The measurements are providing velocity distribution around the wheel and details on bubble and drop distribution.

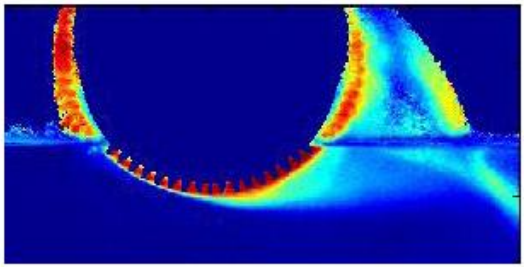

Figure 41: Flow around a spur gear wheel at 100 rpm illustrated by contours of velocity magnitude, showing the oil flow in the air and inside the oil bath.

Figure 42: Model gearbox and gear wheel. Showing the experimental configuration and position of the CCD cameras.

The results of study demonstrate that the flow around the wheel is very complex. The rotation of the wheel results in elevation of the oil by the wheel and creation of the streams of the oil ejecting from the wheel, i.e. the oil splash. The streams can break-up and lead to formation of oil drops. With increased rotation rates the splashed oil streams start to agitate the surface of the oil pool and collide with the gearbox walls. The oil streams entering the oil pool lead to generation of air bubbles in the oil. The penetration of the oil jets into the oil bath and motion of the air bubbles are creating turbulence in the oil.

Base-Flow–Plume Interaction

An experimental flow study of an axisymmetric body in a supersonic stream with an exhaust nozzle operating in the supersonic regime has been performed by means of particle image velocimetry (van Oudheusden and Scarano, 2008). The "FESTIP" (Future European Space Transportation Investigations Programme) model was investigated at free-stream Mach numbers of 2 and 3. The exhaust jet is slightly underexpanded at the nozzle exit at Mach 4. The measurements cover the base region and wake of the model. The PIV technique employs solid submicrometer particle tracers and the particle-image recordings are interrogated with an adaptive multigrid window-deformation technique. The objective of the this work is to provide detailed experimental evidence of the flow topology, by means of particle image velocimetry (PIV). In addition, a validation is made of previous CFD computations (Ottens et al., 2001), carried out with the LORE code developed at the Aerospace Department of Delft University in conjunction with ESA (Walpot, 2002). Figure 43 describes some details of the PIV apparatus installation in the wind tunnel. The integration of PIV in a supersonic wind tunnel requires the consideration of several technical aspects, such as seeding generation and dispersion, particle illumination and recording (Scarano and van Oudheusden, 2000). Fine-grade titanium dioxide (TiO_2) solid particles of 50 nm mean diameter are dispersed in the settling chamber of the wind tunnel, generating a seeded stream of approximately 10 cm diameter in the test section (Figure 43a). The exhaust jet air flow is seeded with the same particle tracers using a high-pressure cyclone generator. The particle tracers' response time is approximately 2 μs, yielding a relaxation length of 1mm. The laser lightsheet, introduced into the test section from downstream, is provided by a Nd:YAG double-cavity laser emitting 400mJ pulses (duration 6 ns) at a rate of 10 Hz. The pulse separation is 1 μs, which allows the particle tracers to travel 0.5mm between pulses. Two CCD cameras (1280×1024 pixels, 12 bit) with interline frame transfer are used to record the particle image pairs. Figures 43b,c show the camera and laser sheet arrangement for the measurements. Two cameras are used to extend the field of view in the wake region (FOV=160×70mm^2).

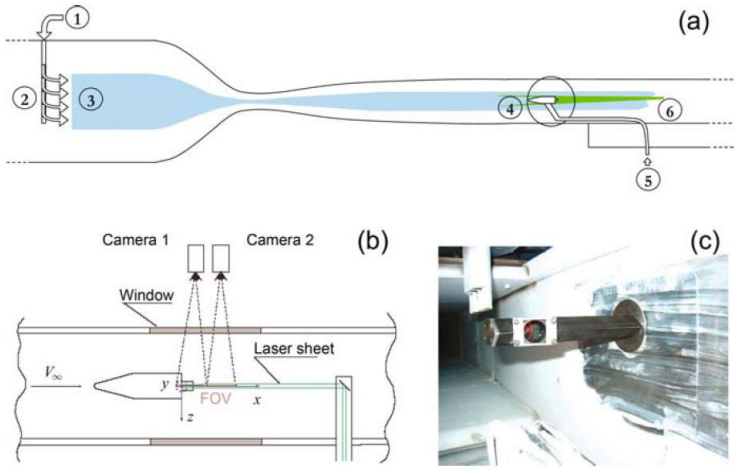

Figure 43: Schematic of the wind tunnel and PIV setup. (**a**) Particle-tracer injection system: 1 seeding inlet, 2 distributor, 3 seeded flow in settling chamber, 4 test section, 5 pressurized air supply line for jet, 6 laser lightsheet; (**b**) two-camera extended view; (**c**) sealed laser-light transmission device .

Figure 44 shows the mean horizontal velocity component and streamlines as obtained by CFD (left) and PIV (right). A good agreement is found on the flow topology, particularly regarding the upper side of the base, where one main recirculation and a saddle point at the base are observed. A similar agreement holds for the flow structure further downstream. Some differences can be detected in the separated flow topology in the region below the nozzle, as well as in the location of maximum reversed flow. Overall, the agreement may be considered acceptable in view of the strong 3D and highly unsteady effect of the model support wake in which case the RANS modeling of turbulence is usually inaccurate.

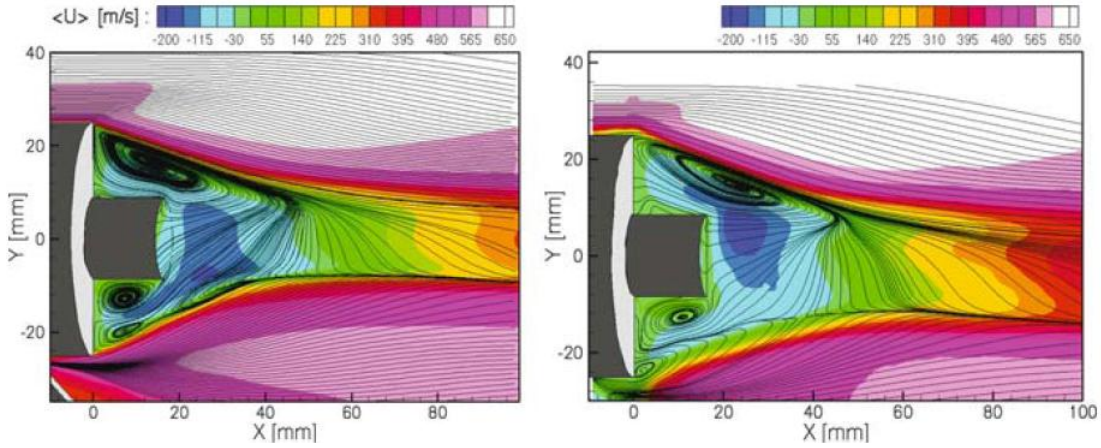

Figure 44: Mean velocity and streamlines pattern at Mach 3 without an exhaust jet. *Left:* CFD. *Right:* experiments.

Concluding remarks

PIV has developed into an effective measurement method, its evolution having been the principal activity of a number of laboratories over the last twenty years. The method is now well established with its limitations and strengths being understood and well documented.

It is risky to predict the future, especially when the advance of PIV depends upon developments in the technology of components that lie outside the field, i.e., computers, lasers, and cameras. However, one can, with some confidence, list developments that would make PIV a more useful and incisive technique (Adrian, 2005):

1. A master theory should be developed that integrates all of the following aspects of PIV:

– Particle dynamics and the relationship between measured particle displacement, particle velocity, and fluid velocity.
– Imaging, including the accuracy and precision of mapping and distortion compensation.
– Image recording and the effect of pixelization with good noise models for the cameras.
– Optimum algorithms for locating particles with maximum accuracy.
– Optimum algorithms for pairing particle images with maximum reliability.
– Interpolating and smoothing regularly sampled data from correlation interrogation or randomly sampled data from particle tracking velocimetry or super-resolution PIV.
2. New, more versatile particle seeding methods are needed to:
– Enable easy optimization of concentration and higher concentrations in large volumes.
– Produce new particles for flows with severe acceleration— e.g., high-drag particles with large scattering cross-sections, such as spiny spheres.
3. The goal should be set to achieve a velocity dynamic range of 1000:1—this would enormously increase the utility of PIV and render tedious optimization of experimental parameters less important.
4. The results of PIV experiments should be held to increasingly rigorous standards. In particular, experimentalists should routinely:
– Demonstrate the adequacy of the spatial resolution by performing grid resolution tests and/or spatial frequency response tests.
– Demonstrate the accuracy and reproducibility of the velocity measurements.
– Routinely examine the probability density histograms of the velocity data for evidence of experimental artifacts.
5. Means should be sought to reduce total system costs by:
– Reducing the costs of light sources and cameras.
– Developing low-cost, restricted-purpose systems, such as probe-PIV.
It is to be emphasized that the importance of PIV as a measurement tool is well recognized and seems likely to continue to find application in stimulating areas of fluid mechanics research.

Acknowledgements

This paper is prepared with the support of Dept. of Fluid Dynamics of Chalmers University and Shiraz University of Technology. The author wish to thank all the researchers whose papers are quoted in this research report and Dr. Valery Chernoray.

References

Abe, M., Yoshida,N., Hishida, K., Maeda, M. (1998) “Multilayer PIV technique with high power pulse laser diodes” in Proc. 9th Int. Symp. Appl. Laser Tech. Fluid Mech. (Instituto Superior T´ecnico, Lisbon, Portugal).

Adrian, R. J. (2005) “Twenty years of particle image velocimetry” Experiments in Fluids, 39, pp. 159–169.

Adrian, R. J. (1986) “Image shifting technique to resolve directional ambiguity in double-pulsed velocimetry”, Appl. Optics, 25, pp. 3855–3858.

Adrian, R. J. (1986) “Multi-point Optical Measurements of Simultaneous Vectors in Unsteady Flow-A Review”, Int. J. Heat Fluid Flow, 7, pp. 127-145.

Adrian, R. J. (1988) “Statistical Properties of Particle Image Velocimetry Measurements in Turbulent Flow” in Laser Anemometry in Fluid Mechanics III, R. J. Adrian, D. F. G. Durao, F. Durst, and J. H. Whitelaw, Eds., pp. 115-129, LADOAN, Instituto Superior Technico, Lisbon.

Adrian, R. J. (1991) “Particle Imaging Techniques for Experimental Fluid Mechanics” Annu. Rev. Fluid Mech., 23, pp. 261-304.

Adrian, R. J. and Yao, C. S. (1985) “Pulsed laser technique application to liquid and gaseous flows and the scattering power of seed materials” Appl. Optics, 24, pp. 44–52.

Adrian, R. J., Christensen, K. T., Liu, Z.-C. (2000) “Analysis and Interpretation of Instantaneous turbulent velocity fields” Exp Fluids, 29, pp. 275-290.

Agüi, J. C., Jiménez J. (1987) “On the performance of particle tracking” J. Fluid Mech., 185, pp. 447-468.

Barnhart, D. H., Adrian, R. J. and Papen, G. C. (1994) “Phase conjugate holographic system for high resolution particle image velocimetry” Appl. Opt., 33, pp. 7159–70.

Bayt, R. L., Breuer K. S. (2001) “Fabrication and testing of micron-sized cold-gas thrusters in micropropulsion of small spacecraft” Advances in Aeronautics and Astronautics, Eds. Micci M. & Ketsdever A., AIAA Press., Washington, D.C. (USA), 187, pp. 381–398.

Boillot, A. and Prasad, A. K. (1996) “Optimization procedure for pulse separation in cross-correlation PIV” Exp. Fluids, 21, pp. 87–93.

Born, M. and Wolf, E. (1970) “Principles of Optics” (Pergamon, Oxford).

Boutier, A., Lefevre, J. B., Micheli, F. (1996) “Analysis of helicopter blade vortex structure by laser velocimetry” Exp. Fluids, 21, pp. 33–42.

Braud, C., Heitz, D., Braud, P., Arroyo, G., Delville, J. (2004) “Analysis of the wake-mixing-layer interaction using multiple plane PIV and 3d classical POD” Exp. Fluids, 37, pp. 95–104.

Brücker C. (1996a) “Spatial correlation analysis for 3-D scanning PIV: simulation and application of dual-color light-sheet scanning” Proc. 89th Intl. Symp. on Laser Techniques to Fluid Mechanics, Lisbon (Portugal).

Brücker, C. (1996b) “3-D PIV via spatial correlation in a color-coded light sheet” Exp. Fluids, 21, pp. 312–314.

Brücker, C. (1997) “3D scanning PIV applied to an air flow in a motored engine using digital high-speed video” Meas. Sci. Technol., 8, pp. 1480–1492.

Brystan-Cross, P. J., Judge, T. R., Quan, C., Pugh, G. and Corby, N. (1995) “The application of digital particle velocimetry (DPIV) to transonic flows” Proc. Aerospace Sci., 31, pp. 1–17.

Buchhave, P. (1992) “Particle Image Velocimetry —Status and Trends”, Experimental Thermal and Fluid Science, 5, pp. 586-604.

Calcagno, G., Di Felice, F., Felli, M., Pereira, F. (2005) “A stereo-PIV investigation of a propeller’s wake behind a ship model in a large free-surface tunnel”, Mar. Technol. Soc. J., 39, pp. 97–105.

Carasone, F., Cenedese, A., Querzoli G. (1995) “Recognition of partially overlapped particle images using the Kohonen neural network” Exp. Fluids, 19, pp. 225–232.

Cenedese, A., and Paglialunga, A. (1987) "A New Approach for the Direct Analysis of Speckle Photograph", LIA, vol. 63, pp. 89-95, ICALEO.

Cenedese, A., and Paglialunga, A. (1990) "Digital Direct Analysis of a Multiexposed Photograph in PIV", Exp. Fluids, 8, pp. 273-280.

Cenedese, A., Querzoli G. (1995) "PIV for Lagrangian scale evaluation in a convective boundary layer" in Flow Visualisation, vol. VI, (eds. Tanida Y, Miyshiro H.), Springer Verlag, Berlin, pp. 863–867.

Chernoray, V., , Sieber, S., Jahanmiri, M. (2011) "PIV Analysis of Flow in a Model Gearbox" 9TH International Symp. on Particle Image Velovimetry–PIV11, Tsukuba, Japan, July 21-23, (to be presented).

Chernoray, V., and Jahanmiri, M. (2011) "Experimental study of multiphase flow in a model gearbox" 6th International Conference on Computational and Experimental Methods in Multiphase and Complex Flow, 15 - 17 June, Kos, Greece, (to be presented).

Cho, Y. C. (1989) "Digital Image Velocimetry", Appl. Opt., 28, pp. 740-748.

Collier, R. J., Burckhardt, C. B. and Lin, L. H. (1971) "Optical Holography" (New York: Academic).

Cotroni, A., Di Felice, F., Romano, G. P., Elefante, M. (2000) "Investigation of the near wake of a propeller using particle image velocimetry" Exp. Fluids, 29, pp. S227– S236 suppl.

Cotroni, A., Di Felice, F., Romano, G. P., Elefante, M. (1999) "Propeller tip vortex analysis by means of PIV" in Proc. 3rd International Workshop on PIV (UCSB, Santa Barbara, US).

Cummings, E. B. (2001) "An image processing and optimal nonlinear filtering technique for PIV of microflows" Exp. Fluids, 29 [Suppl.], pp. 42–50.

Dabiri, D. (2003)"On the interaction of a vertical shear layer with a free surface" J. Fluid. Mech., 480, pp. 217–232.

Di Felice, F., Dolcini, A., Pereira, F., C. Lugni, C. (2005) "Flow survey around the bilge keel of a ship model in free roll decay" in Proc. 6th Int. Symposium on Particle Image Velocimetry (California Institute of Technology, Pasadena, CA, USA).

Di Felice, F., and Pereira, F. (2008) "Developments and Applications of PIV in Naval Hydrodynamics" in A. Schröeder, C.E. Willert (Eds.): Particle Image Velocimetry, Topics Appl. Physics 112, pp. 475–503, Springer-Verlag Berlin Heidelberg.

Di Florio, D., Di Felice, F., Romano, G. P. (2002) "Windowing, re-shaping and reorientation interrogation windows in particle image velocimetry for the investigation of shear flows", Meas. Sci. Technol., 13, pp. 953–962.

Dracos, Th. (1996) "Particle tracking in three-dimensional space" in Three-Dimensional Velocity and Vorticity Measuring and Image Analysis Techniques, ed. Th. Dracos, Kluwer Academic Publishers, Dordrecht (the Netherlands), pp. 209–227.

Dracos, Th. (1996) "Particle tracking velocimetry (PTV) – basic concepts" in Three-Dimensional

Velocity and Vorticity Measuring and Image Analysis Techniques ed. Th. Dracos, Kluwer Academic Publishers, Dordrecht (the Netherlands), pp. 155–160.

Dracos, Th., ed. (1996) "Three-Dimensional Velocity and Vorticity Measuring and Image Analysis Techniques" Kluwer Academic Publishers, Dordrecht (the Netherlands).

Dudderar, T. D., Meynart, R., and Simpkins, P. G. (1988) "Full-Field Laser Metrology for Fluid Velocity Measurement" Opt. Lasers Eng., 9, pp. 163-199.

Elliot G. S., Beutner T. J. (1999) "Molecular filter based planar Doppler velocimetry" Prog. Aero. Sci., 35, pp. 799–845.

Elsinga, G. E., Scarano, F., Wieneke, B., van Oudheusden, B. W. (2006) "Tomographic particle image velocimetry" Exp. Fluids, 41, pp. 933–947.

Gauthier, V. and Riethmuller, M. L. (1988) "Application of PIDV to complex flows: measurement of the third component" VKI Lectures Series on Particle Image Displacement Velocimetry (Brussels) March 1988.

Gaydon, M., Raffel, M., Willert, C., Rosengarten, M., Kompenhans, J. (1997) "Hybrid stereoscopic particle image velocimetry", Exp. Fluids, 23, pp. 331–334.

Gharib, M., Willert, C. E. (1990) "Particle tracing – revisited" in Lecture Notes in Engineering: Advances in Fluid Mechanics Measurements 45, ed. M. Gad-el-Hak, Springer-Verlag, New York, pp. 109–126.

Goss, L. P., Post M. E., Trump D. D., Sarka B. (1989): Two-color particle velocimetry, Proc. ICALEO '89, L.I.A., 68, pp. 101–111.

Grant, I. (1997) "Particle image velocimetry: a review" Proc. Instn. Mech. Engrs., vol. 211, Part C, pp. 55-76.

Grant, I., ed. (1994) "Selected papers on particle image velocimetry" SPIE Milestone Series MS 99, SPIE Optical Engineering Press, Bellingham, Washington.

Grant, I., Liu A. (1990) "Directional ambiguity resolution in particle image velocimetry by pulse tagging" Exp. Fluids, 10, pp. 71–76.

Grant, I., Liu, A. (1989) "Method for the efficient incoherent analysis of particle image velocimetry images" Appl. Optics, 28, pp. 1745–1748.

Grant, I., Pan X. (1995) "An investigation of the performance of multi layer neural networks applied to the analysis of PIV images" Exp. Fluids, 19, pp. 159–166.

Gray, C. and Greated, C. A. (1993) "A processing system for the analysis of particle displacement holograms" Proc. SPIE 2005, pp. 636–47.

Guezennec, Y. G., Brodkey, R. S., Trigui, N., Kent J. C. (1994) "Algorithms for fully automated three-dimensional particle tracking velocimetry" Exp. Fluids, 17, pp. 209–219.

Gui, L., Longo, J., F. Stern, F. (2001) "Towing tank PIV measurement system, data and uncertainty assessment for DTMB model 5512" Exp. Fluids, 31, pp. 336–346.

Göttlich, E., Neumayer, F., Woisetschläger, J., Sanz, W., Heitmeir, F. (2004) "Investigation of stator-rotor interaction in a transonic turbine stage using Laser Doppler Velocimetry and pneumatic probes" ASME J. Turbomach., 126, pp. 297–305.

Göttlich, E., Woisetschläger, J., Pieringer, P., Hampel, B., Heitmeir, F. (2005) "Investigation of vortex shedding and wake-wake interaction in a transonic turbine stage using laser Doppler velocimetry and particle image velocimetry" Proc. ASME Turbo Expo 2005.

Havermann, M., Haertig, J., Rey, C., and George, A. (2008) "PIV Measurements in Shock Tunnels and Shock Tubes" in A. Schröeder, C.E. Willert (Eds.): Particle Image Velocimetry, Topics Appl. Physics 112, pp. 429–443, Springer-Verlag Berlin Heidelberg.

Hinsch, K. (2002) "Holographic particle image velocimetry" Meas. Sci. Tech., 13, pp. R61–R72.

Hinsch, K., Arnold, W., Platen W. (1987) "Turbulence measurements by particle imaging velocimetry" Proc. ICALEO '87—Optical Methods in Flow and Particle Diagnostics, L.I.A., 63, pp. 127–134.

Hinsch, K.D. (1995) "Three-dimensional particle velocimetry" Meas. Sci. Tech., 6, pp. 742–753.

Hu, H., Saga, T. Kobayashi, T., Taniguchi, N., Yasuki, M. (2001) "Dualplane stereoscopic particle image velocimetry: system set-up and its application on a lobed jet mixing flow" Exp. Fluids, 31, pp. 277–293.

Huang, H. T., Fiedler, H. F., Wang, J. J. (1993) "Limitation and improvement of PIV; part II: Particle image distortion, a novel technique" Exp. Fluids, 15, pp. 263–273.

Humble, R. A., Elsinga, G. E., Scarano, F., van Oudheusden, B.W. (2007) "ExperimentalInvestigation of the Three-Dimensional Structure of a Shock Wave/Turbulent Boundary Layer Interaction" 16th Australasian Fluid Mechanics Conference Crown Plaza, Gold Coast, Australia, 2-7 December.

Humble, R. A., Scarano, F. & van Oudheusden, B. W. (2007) "Particle image velocimetry measurements of a shock wave/turbulent boundary layer interaction" Exp. Fluids 43, pp. 173–183.

Humphreys, W. M. (1991) "A Histogram-Based Technique for Rapid Vector Extraction from PIV Photographs" Proc. 4th Int. Conference on Laser Anemometry--Advances and Applications, Cleveland, Ohio, August 1991, pp. 279-283.

Hunter, W. W., Nichols C.E. (1985) "Wind tunnel seeding systems for laser velocimeters" Proc. NASA Workshop, 19–20 March, NASA Langley Research Center (NASA Conference Publication 2393).

Keane, R. D., Adrian, R. J., Zhang, Y. (1995) "Super-resolution particle image velocimetry" Meas. Sci. Tech., 6, pp. 754–768.

Kimura, I. and Takamori, T. (1986) "Image processing of flow around a circular cylinder by using correlation technique" In Flow Visualisation, vol. IV (Ed. C. Veret), pp. 221–226 (Hemisphere, Washington).

Koochesfahani M. M., et al. (1997) "Molecular Tagging Diagnostics for the Study of Kinematics

and Mixing in Liquid Phase Flows, in Developments in Laser Techniques in Fluid Mechanics" R. J. Adrian et al. (eds.), Springer-Verlag, New York, pp. 125–134.

Kähler C. J., Sammler B., Kompenhans J. (2002) "Generation and control of particle size distributions for optical velocity measurement techniques in fluid mechanics" Exp. Fluids, 33, pp. 736–742.

Kähler, C. J. (2003) "General design and operating rules for seeding atomizers" Proc. 5th International Symposium on Particle Image Velocimety, Busan (Korea).

Kähler, C. J., Kompenhans, J. (2000) "Fundamentals of multiple plane stereo particle image velocimetry" Exp. Fluids, 29, pp. S070–S077.

Landreth, C. C., Adrian R. J. (1988): Electrooptical image shifting for particle image velocimetry, Appl. Optics, 27, pp. 4216–4220.

Landreth, C. C., Adrian R. J., Yao C. S. (1988) "Double-pulsed particle image velocimetery with directional resolution for complex flows, Exp. Fluids, 6, pp. 119–128.

Landreth, C. C., and Adrian, R. J. (1988) "Measurement and Refinement of Velocity Data Using High Image Density Analysis in Particle Image Velocimetry", in Applications of Laser Anemometry to Fluid Mechanics, R. J. Adrian, T.Asanuma, D. F. G. Durao, F. Durst, and J. H. Whitelaw, Eds., SPIE, .pp. 484-497, Springer-Verlag, New York.

Lang, H., Mørck, T., Woisetschläger, J. (2002) "Stereoscopic particle image velocimetry in a transonic turbine stage" Exp. Fluids, 32, pp. 700–709.

Lauterborn, W., and Vogel, A. (1984) "Modern Optical Techniques in Fluid Mechanics", Annu. Rev. Fluid Mech., 16, pp. 223-244.

Lim, W. L., Chew, Y. T., Chew, T. C. and Low, H. T. (1994) "Improving the dynamic range of particle tracking veloci metry systems" Exps in Fluids, 17, pp. 282–284.

Lindken, R., Rossi, M., Große, S., and Westerweel, J. (2009) "Micro-Particle Image Velocimetry (μPIV): Recent developments, applications, and guidelines" Lab Chip, The Royal Society of Chemistry, 9, pp. 2551–2567.

Longmire, E. K., Ganapathisubramani, B., Marusic, I., Urness, T. (2001) "Structure Identification and Analysis in Turbulent Boundary Layers by Stereo PIV" 4th International Symposium on Particle Image Velocimetry, Göttingen, Germany, September 17-19.

Lourenco, L. M. and Krothapalli, A. (1989) "Particle velocimetry Advances in Fluid Mechanics Measurements" (Lecture Notes in Engineering) (Berlin: Springer).

Marrett, J. (1967) "Techniques of Modern Photography" (Evans Bros., London).

Martin, P. B., Pugliese, J. G., Leishman, J. G., Anderson, S. L. (2000) "Stereo PIV measurements in the wake of a hovering rotor" Proc. 56th Annual Forum of the American Helicopter Society, Virginia Beach (USA).

Meinhart, C. D. and Zhang, H. S. (2000) "The flow structure inside a microfabricated inkjet printhead" J. MEMS, 9, 67.

Meinhart, C. D., Wereley, S. T., and Gray, M. H. B. (2000) "Volume illumination for two-dimensional particle image velocimetry" Meas. Sci. Technol., 11, pp. 809–814.

Meinhart, C. D., Wereley S. T., Santiago, J. G. (1999) "PIV measurements of a microchannel flow" Exp. Fluids, 27, pp. 414–419.

Melling, A. (1986) "Seeding gas flows for laser anemometry" Proc. AGARD Conference on Advanced Instrumentation for Aero Engine Components, 19–23 May, Philadelphia (USA), AGARD-CP 399-8.

Melling, A. (1997) "Tracer particles and seeding for particle image velocimetry" Meas. Sci. Technol., 8, pp. 1406–1416.

Meng, H., Pan, G., Pu, Y., Woodward, S. C. (2004) "Holographic particle image velocimetry: From film to digital recording" Meas. Sci. Technol., 15, pp. 673–685.

Merzkirch, W. (1987) "Flow Visualization" New York: Academic.

Merzkirch, W., Mrosewski, T. and Wintrich, H. (1994) "Digital particle image velocimetry applied to a natural convective flow". Acta Mechanica, , 4 (Suppl. 1), pp. 19–26.

Meyers J.F., Komine H. (1991) "Doppler global velocimetry – a new way to look at velocity" Proc. ASME Fourth International Conference on Laser Anemometry, Cleveland (USA).

Meyers, J. F. (1991) "Generation of particles and seeding" von Karman Institute for Fluid Dynamics, Lecture Series 1991-05, Laser Velocimetry, Rhode-St-Genese (Belgium).

Mullin J. A., Dahm, W. J. A. (2005) "Dual-plane stereo particle image velocimetry (DSPIV) for measuring velocity gradient fields at intermediate and small scales of turbulent flows", Exp. Fluids, 38, pp. 185–196.

Mullin, J. A., Dahm, W. J. A. (2004) "Direct experimental measurements of velocity gradient fields in turbulent flows via high-resolution frequency-based dual-plane stereo PIV (DSPIV)" Proc. 129th Intl. Symp. on Laser Techniques to Fluid Mechanics, Lisbon (Portugal).

Northrup, M. A., et al. (1995) "A MEMS-based DNA analysis system" Proc. Proceedings of Transducers '95, 8th International Conference on Solid-State Sensors and Actuators, 16–19 June, Stockholm (Sweden), pp. 764–767.

Offutt, P. W. (1995) "Development of experimental technique and studies of spatial structure in turbulent thermal convection" PhD thesis, University of Illinois, Urbana, Illinois.

Okada, E., Enomoto, H., Fukuoka, Y. and Minamitani, H. (1990) "Instantaneous imaging velocimeter with electronic specklegram" In Proceedings of Fifth International Symposium on Applications of Laser Anemometry to Fluid Mechanics, Lisbon, paper 18.2.

Okamoto, K., Hassan, Y. A. and Schmidl, W. D. (1995) "Simple calibration technique using image cross-correlation for three dimensional PIV" Flow Visualization and Image Processing of Multiphase Systems, ed. W. J. Yang et al. (New York: ASME), pp 99–106.

Ottens, H. B. A., Gerritsma, M. I., Bannink, W. J. (2001) "Computational Study of Support Influence on Base Flow of a Model in Supersonic Flow" AIAA paper 2001-2638.

Pereira, F., Costa, T., Felli, M; Calcagno, G:; Di Felice, F. (2003) "A versatile fully submersible stereo-PIV probe for tow tank applications" in Proc. 4th ASMEJSME Joint Fluids Engineering Conference (FEDSM'03), (ASME, Honolulu, HI (USA)).

Pereira, F., Gharib, M. (2002) "Defocusing digital particle image velocimetry and the three-dimensional characterization of two-phase flows" Meas. Sci. Technol., 13, pp. 683–694.

Pereira, F., Stüer, H., Castano-Graff, E., Gharib, M. (2006) "Two-frame 3D particle tracking" Meas. Sci. Technol., 17, pp. 1680–1692.

Prasad, A. K. (2000) "Stereo particle image velocimetry" Exp. Fluids, 29, pp. 103–116.

Prasad, A. K. (2000) "Particle image velocimetry" CURRENT SCIENCE, vol. 79, no. 1, pp. 51-60.

Prasad, A. K., Adrian, R. J. (1993) "Stereoscopic particle image velocimetry applied to liquid flows" Exp. Fluids 15, pp. 49–60.

Prasad, A. K., Adrian, R. J., Landreth, C. C. and Offutt, P. W. (1992) "Effect of Resolution on the Speed and Accuracy of Particle Image Velocimetry Interrogations" Exp. Fluids, 1992, 13, pp. 105–116.

Prasad, A. K., Jensen, K. (1995) "Scheimpflug stereocamera for particle image velocimetry to liquid flows" Appl. Optics, 34, pp. 7092–7099.

Raffel, M., Kompenhans, J. (1993) "PIV measurements of unsteady transonic flow fields above a NACA 0012 airfoil" Proc. 5th Intl. Conf. on Laser Anemometry, Veldhoven (the Netherlands), pp. 527–535.

Raffel, M., Kompenhans, J., Stasicki, B., Bretthauer, B. and Meier, G. E. A. (1995) "Velocity measurement of compressible airflows utilizing a high speed video camera" Exps in Fluids, 18, pp. 204–215.

Raffel, M., Seelhorst, U., Willert, C. (1998) "Vortical flow structures at a helicopter rotor model measured by LDV and PIV" The Aeronautical Journal of the Royal Aeronautical Society, 102, pp. 221–227.

Raffel, M., Willert, C. E., Wereley, S. T., Kompenhans, J. (2007) "Particle Image Velocimetry-A Practical Guide" Springer-Verlag.

Rood, E. P. (ed) (1993) "Holographic particle velocimetry" Proc. Fluids Engineering Division, American Society of Mechanical Engineers, vol 148.

Roth, G., Hart, D. and Katz, J. (1995) "Feasibility of using the L64720 video motion estimation processor (MEP) to increase efficiency of velocity map generation of particl image velocimetry (PIV)" In Laser Anemometry, FEDerrors vol. 229, pp. 387–393 (American Society of Mechanical Engineering, New York).

Royer, H. (2000) "Holography as a 3D PIV method" Proc. EUROMECH 411, Rouen, France.

Royer, H., Stanislas, M. (1996) "Stereoscopic and holographic approaches to get the third velocity component in PIV", von Karman Institute for Fluid Dynamics, Lecture Series 1996–03, Particle Image Velocimetry, Rhode-St-Genése (Belgium).

Röhle I. (1997) “Three-dimensional Doppler global velocimetry in the flow of a fuel spray nozzle and in the wake region of a car” Flow Measurement and Instrumentation, 7, pp. 287–294.

Samimy M., Wernet M. P. (2000) “Review of planar multiple-component velocimetry in high speed flows” AIAA Journal, 38, pp. 553–574.

Santiago, J. G., Wereley, S. T., Meinhart, C. D., Beebe, D. J., Adrian, R. J. (1998) “A particle image velocimetry system for microfluidics” Exp. Fluids, 25, pp. 316–319.

Scarano, F. (2002) “Iterative image deformation methods in PIV” Meas. Sci. Technol., 13, pp. 1–19.

Scarano, F., van Oudheusden, B. W. (2003) “Planar velocity measurements of a twodimensional compressible wake” Exp. Fluids, 34, pp. 430–441.

Siu Y. W., Taylor, A. M. K. P., Whitelaw, J. H. (1994) “Lagrangian tracking of particles in regions of flow recirculation” Proc. 1st Int. Conference on Flow Interaction, Hong Kong, pp. 330-333.

Stanislas, M., Okamoto K., Kähler C. J., Westerweel J. (2005) “Main results of the second international PIV challenge” Exp. Fluids, 39, pp. 170–191.

Stanislas, M., Okamoto, K., Kähler C. J. (2003) “Main results of the first international PIV challenge” Meas. Sci. Tech., 14, pp. R63–R89.

Stasicki, B. and Meier, G. E. A. (1994) “A computer controlled ultra high-speed video camera system” In Proceedings of Twenty-first International Congress on High-speed Photography and Photonics, Taejon, Korea, August 1994, SPIE vol. 2513, pp. 196–208. Elektro. Hochgisch1988 windigkeitskamera, Pat. 42 12271, 1992.

Takai, N., and Asakura, T. (1988) “Displacement Measurements of Speckles using a 2-D Level Crossing Technique” Appl. Opt., 22, pp. 3514-3519.

Törnblom, O. (2004) “Introduction course in particle image velocimetry” [El. doc.].

van der Wall, B. G., Richard, H. (2005) “Analysis methodology for 3C PIV data” Proc. 31st European Rotorcraft Forum, Florence (Italy).

van Doorne, C. W. H., Westerweel, J. (2007) “Measurement of laminar, transitional and turbulent pipe flow using Stereoscopic-PIV” Exp Fluids, 42, pp.259–279.

van Oord, J. (1997) “The design of a stereoscopic DPIV-system” Report MEAH-161 Delft University of Technology, Delft (the Netherlands).

van Oudheusden, B. W., and Scarano, F. (2008) “PIV Investigation of Supersonic Base-Flow–Plume Interaction” in A. Schröeder, C.E. Willert (Eds.): Particle Image Velocimetry, Topics Appl. Physics 112, pp. 465–474, Springer-Verlag Berlin Heidelberg.

Virant, M., Dracos, Th. (1996) “Establishment of a videogrammetic PTV system” in Three-Dimensional Velocity and Vorticity Measuring and Image Analysis Techniques, ed. Th. Dracos, Kluwer Academic Publishers, Dordrecht (the Netherlands), pp. 229–254.

Walpot, L. M. G. F. M. (2002) “Development and application of a hypersonic flow solver” Ph.D. thesis, Delft Univ. Technology.

Wernet, J. H., Wernet M.P. (1994): Stabilized alumina/ethanol colloidal dispersion for seeding high temperature air flows, Proc. ASME Symposium on Laser Anemometry: Advances and Apllications, Lake Tahoe, Nevada (USA), 19–23 June.

Westerweel, J. and Nieuwstadt, S. T. M. (1991) “Performance tests on three-dimensional velocity measurements with a two camera DPIV” Trans. ASME, Laser Anem., 1, pp. 349–355.

Westerweel, J., Nieuwstadt, F.T.M. (1991) “Performance tests on 3-dimensional velocity measurements with a two-camera digital particle-image velocimeter” in Laser Anemometry Advances and Applications, vol. 1 (ed. Dybbs A. and Ghorashi B.), ASME, New York, pp. 349–355.

Westerwell, J. and Niewestadt, F. T. M. (1990) “Measurements of the dynamics of coherent flow structures using particle image velocimetry” In Proceedings of Fifth International Symposium on Applications of Laser Anemometry to Fluid Mechanics, paper 18.3, pp. 476–499 (Springer-Verlag, Berlin, Heidelberg).

Wieneke, B. (2005) “Stereo-PIV using self-calibration on particle images” Exp. Fluids, 39, pp. 267–280.

Willert, C. (1997) “Stereoscopic particle image velocimetry for application in wind tunnel flows” Meas. Sci. Tech., 8, pp. 1465–1479.

Willert, C. E. and Gharib, M. (1991) “Digital particle image velocimetry” Experiments in Fluids, 10, pp. 181-193.

Willert, C. E. and Gharib, M. (1992) “Three-dimensional particle imaging with a single camera” Exp. Fluids, 12, pp. 353–8.

Woisetschläger, J., Lang H., Hampel, B., Göttlich, E., Heitmeir, F. (2003) “Influence of blade passing on the stator wake in a transonic turbine stage investigated by particle image velocimetry and laser vibrometry” Proc. Instn. Mech. Engrs.: J. Power and Energy, 217 A, pp. 385–391.

Woisetschläger, J., Mayrhofer, N., Hampel, B., Lang, H., Sanz, W. (2003a) “Laser-optical investigation of turbine wake flow” Exp. Fluids, 34, pp. 371–378.

Yao, C.-S., and Adrian, R. J. (1984) “Orthogonal Compression and 1-D Analysis Technique for Measurement of 2-D Particle Displacements in Pulsed Laser Velocimetry” Appl. Opt., 23, pp. 1687-1689.

Zhou, J., Adrian, R. J., Balachandar, S., Kendall, T. M. (1999) “Mechanisms for generating coherent packets of hairpin vortices in channel flow”. J. Fluid Mech., 387, pp. 353-359.